Journal of African Earth Sciences 220 (2024) 105458

Contents lists available at ScienceDirect

Journal of African Earth Sciences

journal homepage: www.elsevier.com/locate/jafrearsci

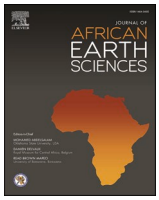

Detrital zircon U-Pb geochronology of the Moatize and N'Condédzi coalfields, Zambezi Karoo Basin of Mozambique: Implications for provenance, sediment dispersal and basin evolution

Paulo Fernandes [a,*], Raul C.G.S. Jorge [b], Luís Albardeiro [c], David Chew [d], Foteini Drakou [d], Zélia Pereira [c], João Marques [e]

[a] CIMA, Centre of Marine and Environmental Research\\ARNET - Infrastructure Network in Aquatic Research, University of Algarve, Campus de Gambelas, 8000-139, Faro, Portugal
[b] IDL - Instituto Dom Luiz, Departamento de Geologia da Faculdade de Ciências, Universidade de Lisboa, Campo Grande, Edifício C6, Piso 4, 1749-016, Lisboa, Portugal
[c] Laboratório Nacional de Energia e Geologia (LNEG), Rua da Amieira, Apartado 1089, 4466-901, S. Mamede de Infesta, Portugal
[d] Department of Geology Trinity College Dublin, Museum Building, Dublin 2, Ireland
[e] Gondwana Empreendimentos e Consultorias, Limitada, Rua 1.335, No. 233, Bairro da COOP, Maputo, Mozambique

ARTICLE INFO

Handling Editor: M Mapeo

Keywords:
Geochronology
Detrital-zircon
Intracontinental extension
Permian-Triassic
Karoo
Mozambique

ABSTRACT

Detrital zircon U-Pb geochronology of the Moatize and N'Condédzi coalfields in the Zambezi Karoo Basin of Mozambique provides key insights into the regional provenance, sediment dispersal pathways and basin evolution. Borehole cores from the two coalfields reveal a stratigraphy spanning the early Roadian (middle Permian) to the Carnian (Upper Triassic). The Permian sandstones of the Moatize Coalfield (MC) yield three detrital zircon populations, with ages ranging from 1150 to 950 Ma, 900–780 Ma and 650–490 Ma. In contrast, the Permian sandstones of the N'Condédzi Coalfield (NC) have only one population, which ranges from 1150 to 950 Ma. During the Permian, the provenance area for the NC was the Tete-Chipata Terrane and Malawi Complex (1150–950 Ma) to the north-northeast. In the MC, the detrital zircon populations of the early lake delta depositional setting (Roadian to Wordian) indicate a main provenance in the Zambezi Belt (900–780 Ma) located to the south of the MC, with minor sourcing from the Nampula Block (1150–950 Ma and 650–490 Ma) to the east. The transition from a lake delta to an alluvial depositional setting is attributed to a major tectonic event in the MC, which involved the formation of a braided channel belt. Sandstones from this braided channel belt yield three detrital zircons populations (650–490 Ma, 900–780 Ma and 1150–950 Ma), indicating provenance from both the Zambezi Belt and the Nampula Block. The overlying sandstones in the MC show only a minor population from the Zambezi Belt (900–780 Ma), implying a shift in provenance to the Nampula Block that was likely induced by tectonics. The absence of detrital zircon populations of 900–780 Ma and 650–490 in the Permian sandstones of NC implies that the two coalfields were not connected during the mid to late Permian. It is likely that an intra-rift horst (the Mesoproterozoic Gabbro-Anorthosite Tete Suite) separated the two coalfields. The Lower Triassic sandstones of the NC yield a main detrital zircon population indicating provenance from the Tete-Chipata Terrane and Malawi Complex (1150–950 Ma). A minor population at 650–490 Ma is linked to increased aridity at the Permian – Triassic boundary, which caused expansion of the watershed across the Tete-Chipata Terrane and the Malawi Complex. The Upper Triassic sandstones in the NC yield a 1150–950 Ma detrital zircon population, indicating provenance from the Tete-Chipata Terrane and Malawi Complex and a return to the source-to-sink conditions seen in the mid to late Permian.

* Corresponding author.
E-mail addresses: pfernandes@ualg.pt (P. Fernandes), rjorge@fc.ul.pt (R.C.G.S. Jorge), luis.albardeiro@lneg.pt (L. Albardeiro), chewd@tcd.ie (D. Chew), drakouf@tcd.ie (F. Drakou), zelia.pereira@lneg.pt (Z. Pereira), joaomarques@gondwana.co.mz (J. Marques).

https://doi.org/10.1016/j.jafrearsci.2024.105458
Received 12 June 2024; Received in revised form 22 October 2024; Accepted 22 October 2024
Available online 26 October 2024

1. Introduction

Detrital-zircon geochronology is an effective tool to obtain insights into the tectonic environment associated with the development of sedimentary basins by identifying source area(s) and sediment dispersal pathways. These can be undertaken when potential source regions have distinct and well-constrained tectonothermal histories (e.g. Barham et al., 2022; Cawood et al., 2012; Dickinson, 2008; Pointon et al., 2012). Detrital zircon geochronology can also be applied to fluvial deposits to gain insight into the source areas of the drainage basin and its reorganisation throughout the evolution of the fluvial system (Midwinter et al., 2024; Song et al., 2022).

This study presents new U-Pb detrital zircon age data from the Moatize and N'Condédzi coalfields of the intracontinental rift Zambezi Karoo Basin of Mozambique (ZKBM). The sedimentary sequences in these two coalfields make a composite continental stratigraphic succession approximately 2 km thick, ranging in age from the Lower Guadalupian to the Carnian. The depositional environment began with a lake delta setting associated with the end Palaeozoic glaciation, shifting to an alluvial depositional setting that persisted from the lower Capitanian (late Guadalupian) until the Carnian. According to Fernandes et al. (2023), the change in depositional setting can be attributed to an important tectonic phase (extensional to transtensional stress along inherited high-strain zones within the Zambezi Mobile Belt, such as the Sanângoè and the Muzarabani Shear Zones), related to the formation of the ZKBM (Fig. 1). This dominantly extensional tectonic regime formed graben and half-graben-type rift basins and lasted throughout the Karoo cycle from the Permian to the Lower Jurassic.

The primary objectives of this research are, therefore, to analyse and interpret the detrital zircon geochronology of the Permian to Triassic continental (lacustrine through alluvial) successions in these two coalfields. Additionally, it aims to determine how tectonic activity

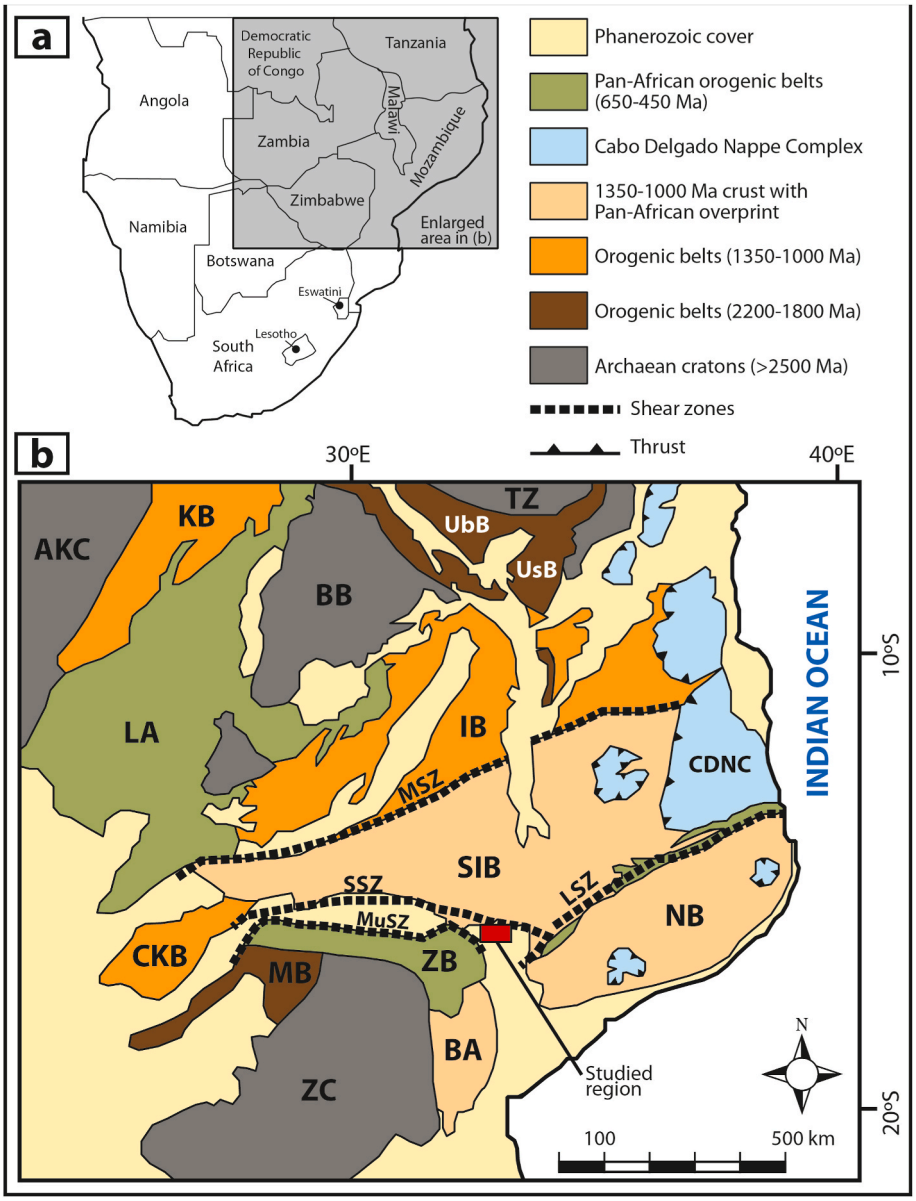

Fig. 1. Simplified map of the principal geotectonic units of Southern East Africa, adapted from Hanson (2003), Bingen et al. (2009), Macey et al. (2013) and Petry et al. (2022). a) Location map. b) Geotectonic map with the main orogenic belts and cratons: AKC – Angola-Kasai Craton, BA – Báruè Complex; BB - Bangweulu Block, CDNC – Cabo Delgado Nappe Complex, CKB – Choma-Kalomo Block, IB – Irumide Belt, KI – Kibaran Belt, LA – Lufillian Arc, MB- Magondi Belt, NB – Nampula Block, SIB – Southern Irumide Belt, TZ – Tanzania Craton, UbB – Ubendian Belt, UsB – Usagaran Belt, ZB – Zambezi Belt, ZC – Zimbabwe Craton. Dashed lines are ductile shear zones: LSZ – Lúrio Shear Zone (=Lúrio Belt), MSZ – Mwembeshi Shear Zone, MuSZ – Muzarabani Shear Zone, SSZ – Sanângoe.

contributed to the formation of the Karoo sedimentary fill architecture, including the principal coal deposition periods. Furthermore, the study of the detrital zircon geochronology seeks to investigate the development of these Karoo depocenters over time by examining changes in drainage patterns in response to tectonic events, and significant environmental changes that occurred across the Permo-Triassic boundary.

The Moatize and N'Condédzi coalfields are bounded by terranes that contain rocks from various crustal growth events and orogenies dating from the Mesoproterozoic to the Early Palaeozoic (see Fig. 1). The ages

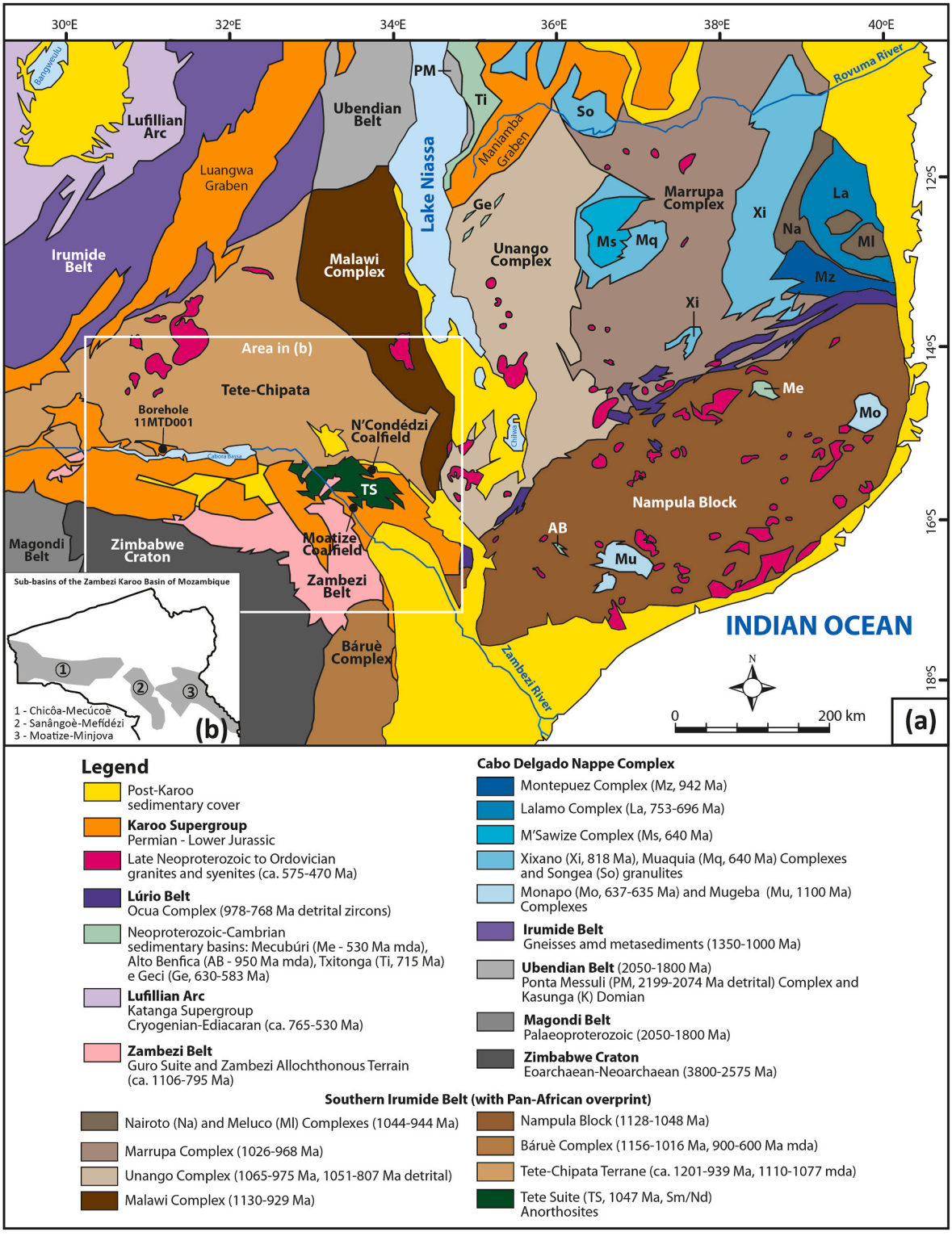

Fig. 2. (a) Detailed geological map depicting the geotectonic units of the various orogenic belts and cratons surrounding the Zambezi Karoo Basins in Mozambique, the location of the Moatize and N'Condédzi coalfields and the location of borehole 11MTD001 of Whitecross (2020). The magmatic ages of the various geotectonic units are employed otherwise stated (mda – maximum deposition age of detrital zircons). **(b)** The position of the three Karroo sub-basins that compose the Zambezi Karoo Basin of Mozambique. Adapted from Bingen et al. (2009), Macey et al. (2013) and Goscombe et al. (2020).

of their magmatic and metamorphic events are well-determined, providing crucial data for a thorough source-to sink analysis of the clastic sediments in these coalfields. To the south of the coalfields, the geology consists of the Zimbabwe Craton, part of the great Kalahari Craton, and the surrounding Proterozoic to early Palaeozoic mobile belts, namely the Zambezi Belt, Magondi Belt Choma-Kaloma Block, Nampula Block and Báruè Block (Goscombe et al., 2020; Hanson, 2003). To the north and east, the coalfields are bordered by Meso-Neoproterozoic mobile belts belonging to the Southern Irumide Belt, the Irumide Belt, the Cabo Delgado Nappe Complex and the Lufilian Arc (Bingen et al., 2009; Chaúque et al., 2019; Hanson, 2003; Johnson et al., 2006; Macey et al., 2010). The oldest terranes to the north comprise the Palaeoproterozoic Bangweulu Block and the Mesoproterozoic (2200 Ma to 1800 Ma) Ubendian - Usagaran Belts (Fig. 1).

2. Geological background

Mozambique's most representative and studied Karoo sedimentary depocenters are located along the Zambezi River valley in the Province of Tete, in northwest Mozambique (Fig. 2). Tectonic reactivation under extensional and transtensional stress of high-strain zones of the Zambezi Mobile Belt, a part of the Pan-African Orogeny (570–530 Ma), during Permian – Triassic times, formed a system of continental graben and half-graben-type rift basins known as the ZKBM (Afonso, 1984; Afonso et al., 1998; Bicca et al., 2017; GTK Consortium, 2006; Orpen et al., 1989). The formation of the ZKBM is believed to be linked to the movements of an original Tethyan spreading center along the northern edges of Gondwana and the propagation of this extensional regime into central and southern Gondwana (Catuneanu et al., 2005). The extensional movements progressed gradually, creating rift basins that became progressively younger from north to south. For instance, the Karoo deposition in the Ruhuhu Basin in Tanzania began in the late Carboniferous (e.g. Wopfner et al., 2009). In contrast, in the Moatize Coalfield, Karoo deposition began during the late Cisuralian (Fernandes et al., 2023).

In the Karoo intracontinental rift basins, several tectonic pulses are recognised and described, related to normal faulting along the rift's master and antithetic faults. Faulting uplifted the rift shoulders that acted as the main sediment sources transported and deposited in the graben depocentres. Usually, the tectonic pulses correspond to the main phases of normal faulting and are recognised in the sedimentary record by an increase in the clastic sediment load of the alluvial settings, forming thinning and finning upward alluvial cycles. These alluvial cycles may start at the base with coarse-grained conglomerates and sandstone deposited in braided channel belts, which progressively pass upward to meandering channel belts (Verniers et al., 1989; Fernandes et al., 2023). The successive fault movements in these rift basins controlled, therefore, the sediment accommodation space and the vertical organisation of the lacustrine and alluvial sedimentary deposits that progressively filled the basin depocentres.

The ZKBM is divided into three sub-basins, which are from east to west: i) the Moatize-Minjova Sub-Basin, ii) the Sanângoè-Mefidéze Sub-Basin, and iii) the Chicôa-Mecúcoè Sub-Basin (Hartzer et al., 2008) (Fig. 2). One of the main features of the Lower Karoo sedimentary successions in these sub-basins is their extensive mid to upper Permian coal seams and their associated coalfields (Vasconcelos and Achimo, 2010). This detrital U-Pb zircon study exclusively concerns the sedimentary successions of the Moatize and N'Condédzi coalfields of the Moatize-Minjova Sub-Basin (Fig. 2), the most intensively explored and exploited sub-basin of the ZKBM.

The studied sandstones were sampled from eight coal exploration boreholes, five in the Moatize Coalfield and three in the N'Condédzi

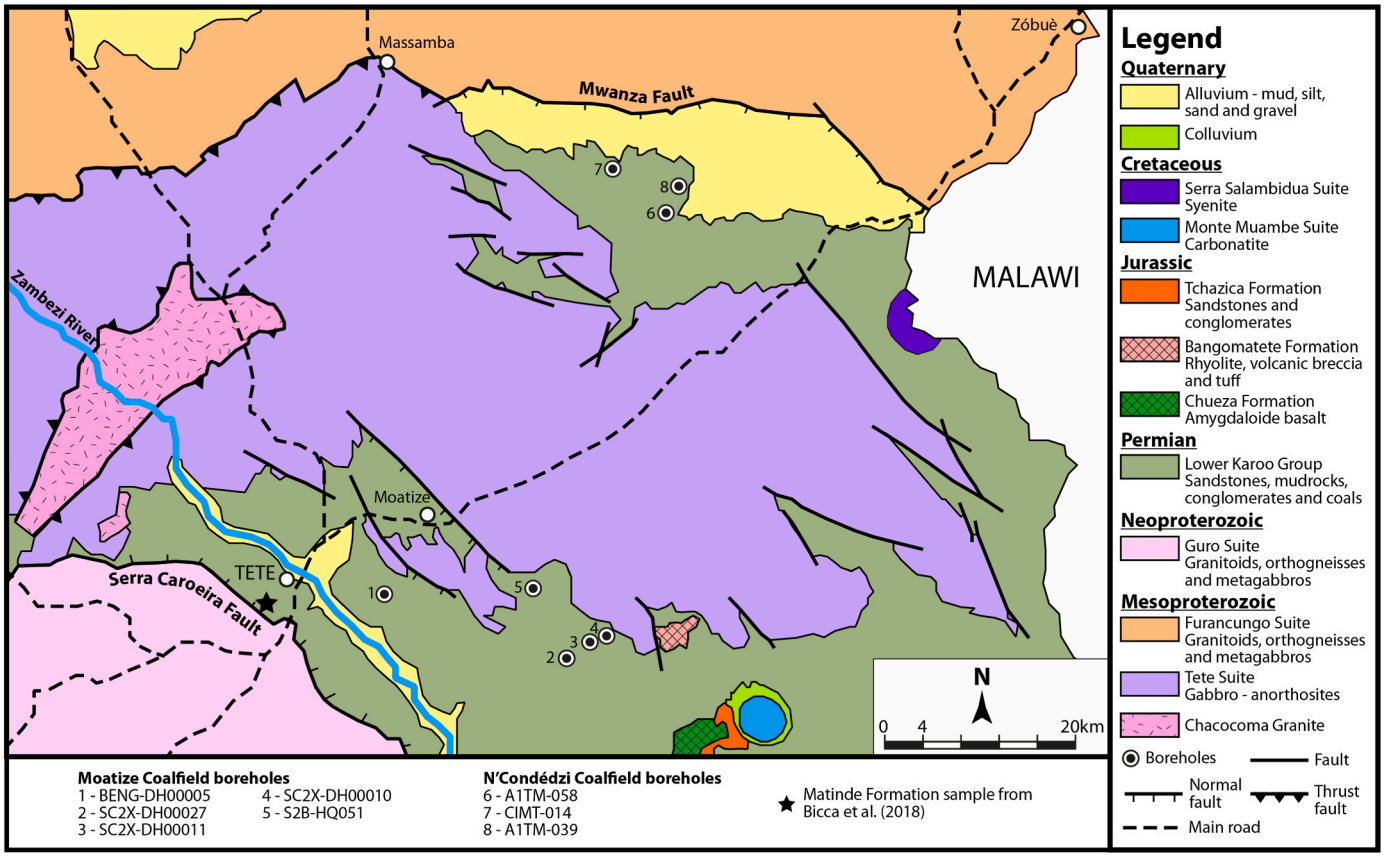

Fig. 3. Detailed geological map of the Moatize and N'Condédzi coalfields with studied boreholes marked. Adapted from Geological Map of Mozambique, Sheet No. 1533/1534, Cazula/Zóbuè, and Sheet No. 1633, Tete, Geological Series 1/250,000, Direcção Nacional de Geologia, Maputo (2006).

Coalfield (Fig. 3). The palynological ages of the eight boreholes indicate a composite stratigraphy encompassing a succession from late Cisuralian-early Guadalupian to early Late Triassic (Carnian) times, with a hiatus in the Middle Triassic (Fernandes et al., 2023; Galasso et al., 2019b).

The Moatize and N'Condédzi coalfields are located on opposite sides of the Moatize-Minjova Sub-Basin and are in faulted contact with basement rocks. To the southwest, the Moatize Coalfield is separated from the Zambezi Belt and Báruè Block by the Serra Caroeira Fault, while to the north, the N'Condédzi Coalfield is separated from the Southern Irumide Belt by the Mwanza Fault (Fig. 3). These last two faults are considered the main faults in the coalfields and experienced the majority of the fault displacements during the deposition of the Karoo sediments. The basement rocks bounded by these faults constituted the rift shoulders and were the potential source areas for the sediments that progressively filled the grabens.

The two coalfields are separated by extensive outcrops of gabbro-anorthosites belonging to the Mesoproterozoic Tete Suite (Fig. 3). As a result of the half-graben to graben geometry of the rift basins, the Karoo sequences in the two coalfields exhibit varying thicknesses, thickening towards the Serra Caroeira and Mwanza faults and thinning towards the Tete Suite, where they overlap it (Fernandes et al., 2023; Lopes et al., 2021a, 2021b; Galasso et al., 2019b).

The lower Karoo Supergroup in the Moatize-Minjova Sub-Basin comprises four clastic units, which are, from base to top: the Vúzi, Moatize, Matinde and Cádzi formations (GTK Consortium, 2006a). The Vúzi Formation unconformably overlays the Mesoproterozoic gabbros and anorthosites of the Tete Suite (Sm-Nd whole rock isochron of 1025 ± 79 Ma, Evans et al., 1999). The Vúzi Formation consists of clast-to matrix-supported conglomerates, sandstones, siltstones, carbonaceous mudstones and coals, and it has been interpreted as representing a fluvial to lacustrine setting (Achimo et al., 2014; Pendkar et al., 2014), and more specifically a lake delta environment in a periglacial setting (Fernandes et al., 2023) related to the end of the Late Palaeozoic Glaciation. In the Moatize Coalfield, the Vúzi Formation is late Kungurian to early Roadian age (Fernandes et al., 2023; Galasso et al., 2019a; Lopes et al., 2021a; Pereira et al., 2016, 2019). The Vúzi Formation is not seen in the N'Condédzi Coalfield, as neither its characteristic lithofacies nor palynomorphs of late Kungurian to early Roadian age have been identified (Galasso et al., 2019b).

The Moatize Formation conformably overlies the Vúzi Formation. The boundary between the two formations is usually placed above the last conglomerate bed in the Vúzi Formation. However, in a lake delta depositional setting, conglomerates would not be found in distal lake floor sub-environments, and the boundary between the two formations is thus uncertain in the distal facies (Fernandes et al., 2023). The Moatize Formation comprises workable coal seams of variable thicknesses intercalated with coarse-to fine-grained micaceous sandstones, siltstones, mudstones and rare matrix-supported conglomerates. The coal seams in the Moatize Formation are termed the Sousa Pinto, Chipanga, Bananeiras, Intermédia and Grande Falésia from oldest to youngest. The post-glacial Moatize Formation represents a shallow lacustrine setting at the base to fluvial braided river settings in the middle and upper parts of the formation. The change from the lacustrine to fluvial deposition is attributed to an important regional tectonic phase that tilted the basin floor to the west and uplifted the watershed that occurred after the deposition of the Chipanga Seam (Fernandes et al., 2023). The Moatize Formation in the Moatize Coalfield spans the late Roadian to late Wuchiapingian (early Guadalupian to mid-Lopingian), with the change from lacustrine to fluvial depositional constrained to the early Capitanian (Fernandes et al., 2023).

The Matinde Formation conformably overlies the Moatize Formation and comprises coarse-to fine-grained sandstones, siltstones, mudstones, coal beds and conglomerates. The sandstone beds occur as isolated or amalgamated beds and show sedimentary features suggesting fluvial channel fill deposits. The mudrock lithologies and coal horizons (André and several unnamed coal seams) correspond to floodplain deposits within these fluvial systems. The absence of thick coal seams and abundance of laminae and thin beds of barcode coal are the main differences between the Matinde Formation and the underlying Moatize Formation (Fernandes et al., 2023; Lopes et al., 2021b). However, as the formations are petrographically similar, the boundary between the two formations can be difficult to recognise. In the Moatize Coalfield the boundary is placed above the Grande Falésia Coal Seam, at the base of an amalgamated package of coarse-to medium-grained sandstone beds interpreted as a renewed phase of regional tectonic uplift linked to the development of a new braided channel belt. In the Moatize coalfield, the Matinde Formation is of Changhsingian age (Late Lopingian) and is defined by the first occurrence (FO) of the *Osmundacidites senectus* miospore (Pereira et al., 2019; Fernandes et al., 2023). This correlates with the L3 palynological assemblage described in the N'Condédzi Coalfield and constrains the age of the Matinde Formation from the early Changhsingian up to the Permo-Triassic boundary (Galasso et al., 2019b). The Matinde Formation reaches a maximum thickness of ca. 2 km (GTK Consortium, 2006a).

The Cádzi Formation is the last unit of the Karoo succession. It consists of red-brown coarse-to medium-grained arkosic sandstones interbedded with red-, green- and buff-coloured siltstones and mudstones. The sandstones show normal grading and large-scale cross-bedding and represent a channel-fill succession of braided rivers, while the siltstones and mudstones represent overbank deposits (GTK Consortium, 2006a). The Cádzi Formation was recognised only in two boreholes (CIMT-014 and A1TM-039) of the N'Condédzi Coalfield in this study. It is Lower Triassic (Induan) to Upper Triassic (Carnian) in age, with a depositional hiatus in the Middle Triassic (Galasso et al., 2019b). In the N'Condédzi Coalfield, the Cádzi Formation has a minimum thickness of ca. 1.2 km (Galasso et al., 2019b).

3. Materials and methods

Detrital zircons were extracted from sandstones from eight coal exploration boreholes in the Moatize (five boreholes) and N'Condédzi (three boreholes) coalfields of the Moatize-Minjova Sub-Basin (Fig. 3), to characterise the source terranes of these two depocenters on opposite sides of the Moatize-Minjova Sub-Basin. Table 1 provides a summary description of the stratigraphic succession of the two coalfields, the stratigraphic age of the samples and their depositional environment. Appendix 2 shows examples of the sandstones that were sampled from the N'Condédzi Coalfield.

Figs. 4 and 5 display the location of the samples in the stratigraphic succession of the boreholes and their correlation with depositional environments identified in both coalfields. The interpretation of the sedimentary environments in the Moatize Coalfield is after Fernandes et al. (2023), and in the N'Condédzi Coalfield is after Galasso et al. (2019a,b). Photographs of the N'Condédzi Coalfield borehole cores, where some of the sandstones were collected, are provided in the supplementary material.

In the Moatize Coalfield (Fig. 4), the samples were collected: i) from below the late Wordian Chipanga Seam, which represents the earliest sedimentary infill in a lake delta setting; ii) the first braided channel belt above the Chipanga Seam associated with a major tectonic pulse linked to the shift from a lake delta to alluvial depositional setting; iii) above the first braided channel belt and below the late Wuchiapingian Grande Falésia Seam, and iv) above the Grande Falésia Seam representing the second braided channel belt.

In the N'Condédzi Coalfield (Fig. 5), deposition began in the early Capitanian with the Wordian and Roadian age sediments missing, and this hinders the correlation of the Permian depositional facies with the Moatize Coalfield. Therefore, for the Guadalupian to Lopingian succession of borehole A1TM-058, the stratigraphic position of the Chipanga and Grande Falésia seams was based on the position of the two prominent braided channel belts identified using the same palynological

Table 1
Summary of the stratigraphic succession of the two coalfields, the stratigraphic age of the samples and their depositional environment after Fernandes et al. (2023) for the Moatize Coalfield and Galasso et al. (2019b) for the N'Condédzi Coalfield.

Moatize Coalfield						
Borehole	Sample ref.	Depth (m)	Formation	Age	Depositional phase	Notes
BENG-DH00005	E81	102	Matinde	Changhsingian	Alluvial Plain	Second braided channel belt
	LD21	245	Moatize	Wuchiapingian	Alluvial Plain	Between braided channel belts
	LD20	522	Moatize	Capitanian	Alluvial Plain	First braided channel belt
	E79	780	Vúzi	Roadian	Lake delta	Deglacial phase
SC2X-DH00027	B03	329.6	Moatize	Changhsingian	Alluvial Plain	Second braided channel belt
	B02	488.1	Moatize	Capitanian	Alluvial Plain	First braided channel belt
	B01B	624.4	Vúzi	Roadian	Lake delta	Deglacial phase
	B01A	635.5	Vúzi	Roadian	Lake delta	Deglacial phase
SC2X-DH00010	A63	12.3	Matinde	Changhsingian	Alluvial Plain	Second braided channel belt
	A62	315.7	Moatize	Wordian	Lake delta	Base Chipanga seam
SC2X-DH00011	D34	65.6	Matinde	Changhsingian	Alluvial Plain	Second braided channel belt
	D33	344.2	Moatize	Wordian	Lake delta	Base Chipanga seam
S2B-HQ051	C23	23	Matinde	Changsingian	Alluvial Plain	Second braided channel belt
N'Condédzi Coalfield						
Borehole	**Sample ref.**	**Depth (m)**	**Formation**	**Age**	**Depositional phase**	**Notes**
A1TM-058	LD3	102	Matinde	Changhsingian	Alluvial Plain	Meandering belt
	LD60	251	Matinde	Changhsingian	Alluvial Plain	Meandering belt
	LD22	591	Matinde	Wuchiapingian	Alluvial Plain	Second braided channel belt
	LD2	796	Moatize	Wuchiapingian	Lake delta	First braided channel belt
	LD58	833	Moatize	Wuchiapingian	Lake delta	Meandering belt
CIMT-014	LD13	130	Cádzi	Carnian	Alluvial Plain	Meandering belt
	LD17	143	Cádzi	Olenekian	Alluvial Plain	Meandering belt
	LD15	256	Cádzi	Olenekian	Alluvial Plain	Braided channel belt
	LD12	310	Cádzi	Olenekian	Alluvial Plain	Meandering belt
	LD16	355	Cádzi	Induan	Alluvial Plain	Braided channel belt
	LD19	434	Cádzi	Induan	Alluvial Plain	Braided channel belt
	LD11	460	Cádzi	Induan	Alluvial Plain	Braided channel belt
	LD14	500	Matinde	Changhsingian	Alluvial Plain	Last Permian sandstone
A1TM-039	LD10	96	Cádzi	Carnian	Alluvial Plain	Braided channel belt
	LD9	554	Cádzi	Carnian	Alluvial Plain	Meandering belt

criteria for the Moatize Coalfield as described in Fernandes et al. (2023). The shift from a lake delta to an alluvial setting was tentatively placed above sample A1TM-058/LD58. Samples A1TM-058/LD2 and A1TM-058/LD22 in this borehole represent the two braided channel belts, and the remaining Permian sandstone samples (LD60 and LD3) represent the channel-fill of meandering river systems. For the Triassic succession, sandstones were sampled from thick sandstone intervals representing high-energy fluvial pulses related to tectonism and across prominent stratigraphic boundaries recognised in the succession (i.e., the Permo-Triassic and Lower – Upper Triassic boundaries).

3.1. Laboratory and analytical methodology

All drill core samples underwent a standard separation process for heavy minerals (Mange and Maurer, 1992) in the LNEG Lab facilities in Portugal. This included crushing and sieving to 40–250 μm, followed by density (Wilfley Table), magnetic (Frantz), and heavy liquid (poly-tungstate) separation. After individual grains were hand-picked under a Zeiss Stemi SV6 binocular microscope, zircons were mounted in epoxy resin, ground to half-thickness and then polished.

Detrital zircon grains underwent U-Th-Pb isotopic analyses at the Department of Geology, Trinity College Dublin, Ireland. A Photon Machines Iridia 193 nm ArF excimer laser-ablation system with a Cobalt 2-vol ablation cell, coupled to an Agilent 7900 mass spectrometer was employed. Line scans on NIST612 standard glass were used to tune the instrument, by obtaining a Th/U ratio close to unity and low oxide production rates (i.e., ThO^+/Th^+ typically <0.15%). A circular laser spot of 24 μm was employed with the spot diameter constant for each session. A repetition rate of 13 Hz and a fluence of 2.25 J cm^{-2} was employed. The helium carrier gas was fed into the laser cell at ~0.4 l min^{-1}, and was mixed with ~0.6 l min^{-1} Ar make-up gas and 11 ml min^{-1} N_2. Each analysis comprised 27.3 s of ablation (300 shots) and 12 s of washout time and the latter portions of the washout were used for baseline measurements. The data reduction of raw U-Th-Pb isotopic data was undertaken using the freeware IOLITE package (Paton et al., 2011) using the "VizualAge" data reduction scheme (Petrus and Kamber, 2012). Conventional sample-standard bracketing was then applied to account for both downhole fractionation and long-term drift in isotopic or elemental ratios by normalising all ratios to those of the U-Th-Pb reference materials. For the Moatize Coalfield samples, the primary U-Pb zircon calibration standard was Plešovice zircon (^{206}Pb-^{238}U age of 337.13 ± 0.37 Ma; Sláma et al., 2008). The secondary standards were GZ7 zircon (^{206}Pb-^{238}U TIMS age of 530.26 Ma ±0.05 Ma; Nasdala et al., 2018) which yielded a ^{206}Pb-^{238}U weighted mean age of 532.9 ± 1.0 Ma (n = 180; MSWD = 0.94), and WRS 1348 zircon (^{206}Pb-^{238}U age of 526.26 ± 0.70; Pointon et al., 2012) which yielded a ^{206}Pb-^{238}U weighted mean age of 523.3 ± 1.4 Ma (n = 134; MSWD = 0.99). For the N'Condédzi Coalfield samples, the primary U-Pb zircon calibration standard was 91500 zircon (^{206}Pb-^{238}U age of 1065.4 ± 0.6 Ma; Wiedenbeck et al., 1995; Wiedenbeck et al., 2004). The secondary standards were Plešovice zircon, which yielded a ^{206}Pb-^{238}U weighted mean age of 339.5 ± 1.2 Ma (n = 119; MSWD = 2.0), and GZ-7 zircon, which yielded a ^{206}Pb-^{238}U weighted mean age of 533.9 ± 1.4 Ma (n = 117; MSWD = 0.98).

Data plotting was carried out using Isoplot 3.0 software (Ludwig, 2003) for concordia diagrams and probability density plots (Figs. 6 and 7). The Density Plotter Java application was used for Kernel Density estimation and Probability Density plotting (Vermeesch, 2012). Concordia ages (concordant data only) were used for all ages quoted in the text and for all grains on the probability density plots (Figs. 6 and 7). The

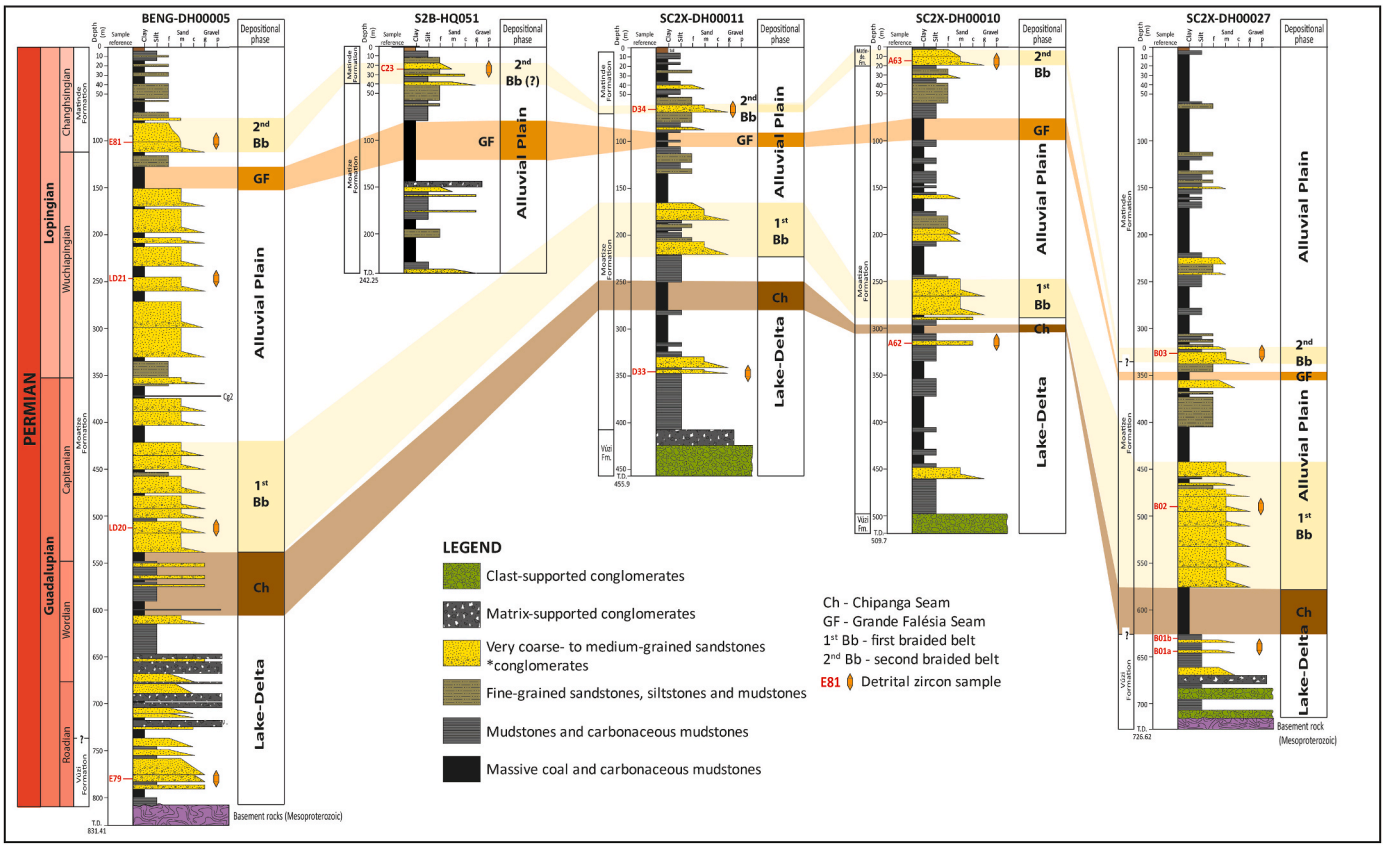

Fig. 4. Stratigraphic logs of the Moatize Coalfield boreholes showing depositional environments, their correlation across the coalfield and the stratigraphic position of the samples. Adapted from Fernandes et al. (2023).

U–Pb LA-ICP-MS data are shown in the appendix files.

4. U-Pb geochronology results

Tables 2 and 3 summarise U-Pb geochronology results, including the ages of the oldest and youngest zircon grains, the main age population peaks, and the modal percentages of grain ages falling within geological periods. Individual U-Pb detrital zircon ages for all samples are provided in the supplementary material.

The following section summarises the results according to the stratigraphic position of the samples. For the Moatize Coalfield and borehole A1TM-058 (N'Condédzi Coalfield), the stratigraphic position is determined relative to the Chipanga and Grande Falésia seams. For the other two boreholes in the N'Condédzi Coalfield, the results are presented according to the sub-environments of the alluvial plain setting (channel-fill of braided or meandering river systems).

4.1. Moatize Coalfield (Fig. 6, Table 2)

4.1.1. Lake delta depositional phase - Vúzi Formation and Moatize Formation (below the Chipanga Seam)

The samples from this depositional phase are from boreholes SC2X-DH00027 (B01A and B01B), SC2X-DH00010 (A62), SC2X-DH00011 (D33) and BENG-DH00005 (E79). The sandstones represent deposition within a lake delta setting during the deglacial phase that followed the late Palaeozoic Gondwana glaciation.

The samples from the Vúzi Formation are characterised by two distinct subpopulations. The first (and main) subpopulation exhibits ages clustering between 920 and 750 Ma, with peaks at ca. 882 Ma, 844 Ma and 830 Ma. The second subpopulation is in the range of 598–494 Ma, with peaks at ca. 560 Ma, 540 Ma and 536 Ma. Accordingly, the detrital zircons are predominately of Neoproterozoic (Tonian) age, followed by Cambrian age detrital zircons.

The Moatize Formation samples in this depositional phase yield broader U-Pb-age zircon spectra than the Vúzi Formation. In sample SC2X-DH00011/D33, most U-Pb ages of the zircon grains fall within 901–762 Ma, with a peak at ca. 871 Ma. Additionally, two smaller subpopulations are present at 1049–959 Ma (peak at 1034 Ma) and 565–493 Ma (peak at 553 Ma). Neoproterozoic ages (68% Tonian, 5% Cryogenian and 5% Ediacaran) predominate in this sample, with subordinate Mesoproterozoic (18%) and Cambrian zircons (5%).

Zircons in sample SC2X-DH00010-A62 are Mesoproterozoic (36%), Neoproterozoic (36%) and Cambrian (24%), with occasional Paleoproterozoic and Ordovician zircons. U-Pb ages can be grouped into two subpopulations. The first subpopulation has an age range of 576–487 Ma, with a peak at ca. 500 Ma and a smaller peak at ca. 560 Ma. The second subpopulation ranges between 1048 and 954 Ma, with a main peak at 1015 Ma and smaller peaks at 1067 Ma and 969 Ma. Additionally, a much smaller subpopulation was found at 908–730 Ma, with a peak at 804 Ma.

There is, therefore, an increase in Mesoproterozoic zircons and a decrease in Neoproterozoic zircons in the Vúzi to the Moatize formations. Cambrian zircons are the only subpopulation found in all these samples.

4.1.2. Alluvial plain depositional phase – Moatize Formation (first braided channel belt above the Chipanga Seam)

The two samples from the older braided channel belt, BENG-DH00005/LD20 and SC2X-DH00027/B02, yielded detrital zircons with broad age spectra, showing three subpopulations. The zircons from sample BENG-DH00005/LD20 yield three subpopulations at 1070–1000 Ma, 850–770 Ma and 600–477 Ma. The most prominent

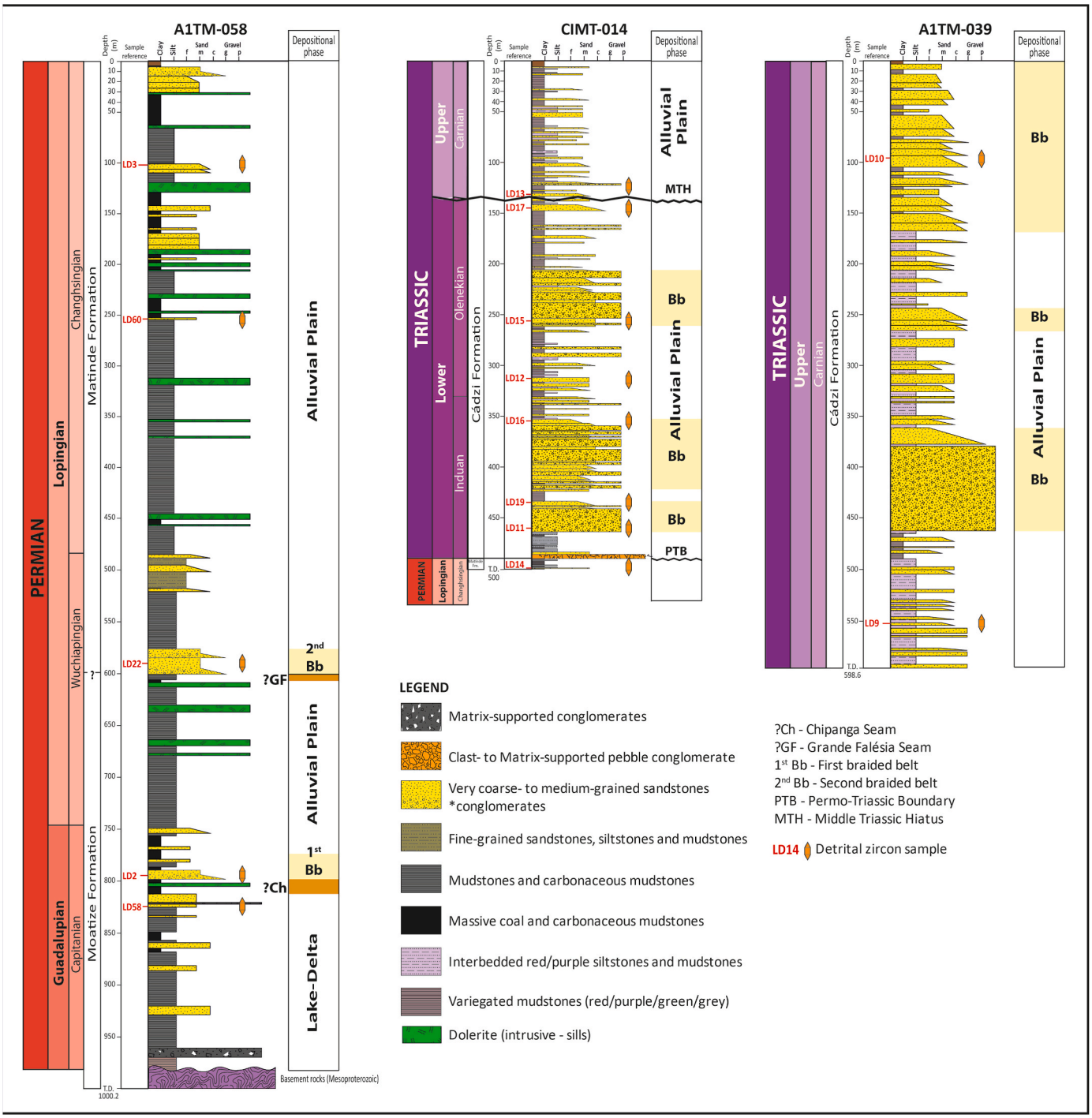

Fig. 5. Stratigraphic logs of the N'Condédzi Coalfield boreholes showing depositional environments, their correlation across the coalfield and the stratigraphic position of the samples. Adapted from Galasso et al. (2019b).

peak occurs at ca. 1040 Ma, while secondary peaks are at 928 Ma, 844 Ma, 785 Ma, 700 Ma, 598 Ma, 526 Ma and 477 Ma. Detrital zircon ages in sample SC2X-DH00027/B02 can also be divided into three subpopulations at 1143–956 Ma, 880–812 Ma and 577–502 Ma, with peaks at 1104 Ma, 860 Ma and 534 Ma, respectively. Sample BENG-DH00005-LD21 above the older braided channel belt is characterised by two detrital zircon subpopulations, one ranging from 578 to 481 Ma, with a peak at ca. 517 Ma and a second at 1139–949 Ma, with two peaks at ca. 1043 and 1091 Ma.

4.1.3. Alluvial plain depositional phase - Matinde Formation (second braided channel belt, above the Grande Falésia seam)

Five sandstone samples (BENG-DH00005/E81, S2B-HQ051/C23, SC2X-DH00011/D34, SC2X-DH00010/A63, and SC2X-DH00027/B03) from the second braided channel belt were analysed. All samples except BENG-DH00005/E81 showed two age subpopulations. The main subpopulation is of Mesoproterozoic age at 1166–923 Ma. The second subpopulation is Cambrian to Neoproterozoic age (690–464 Ma). Sample BENG-DH00005/E81 yielded three zircon subpopulations, including the two subpopulations mentioned above and a third subpopulation at 899–836 Ma. This third subpopulation is commonly found in samples of

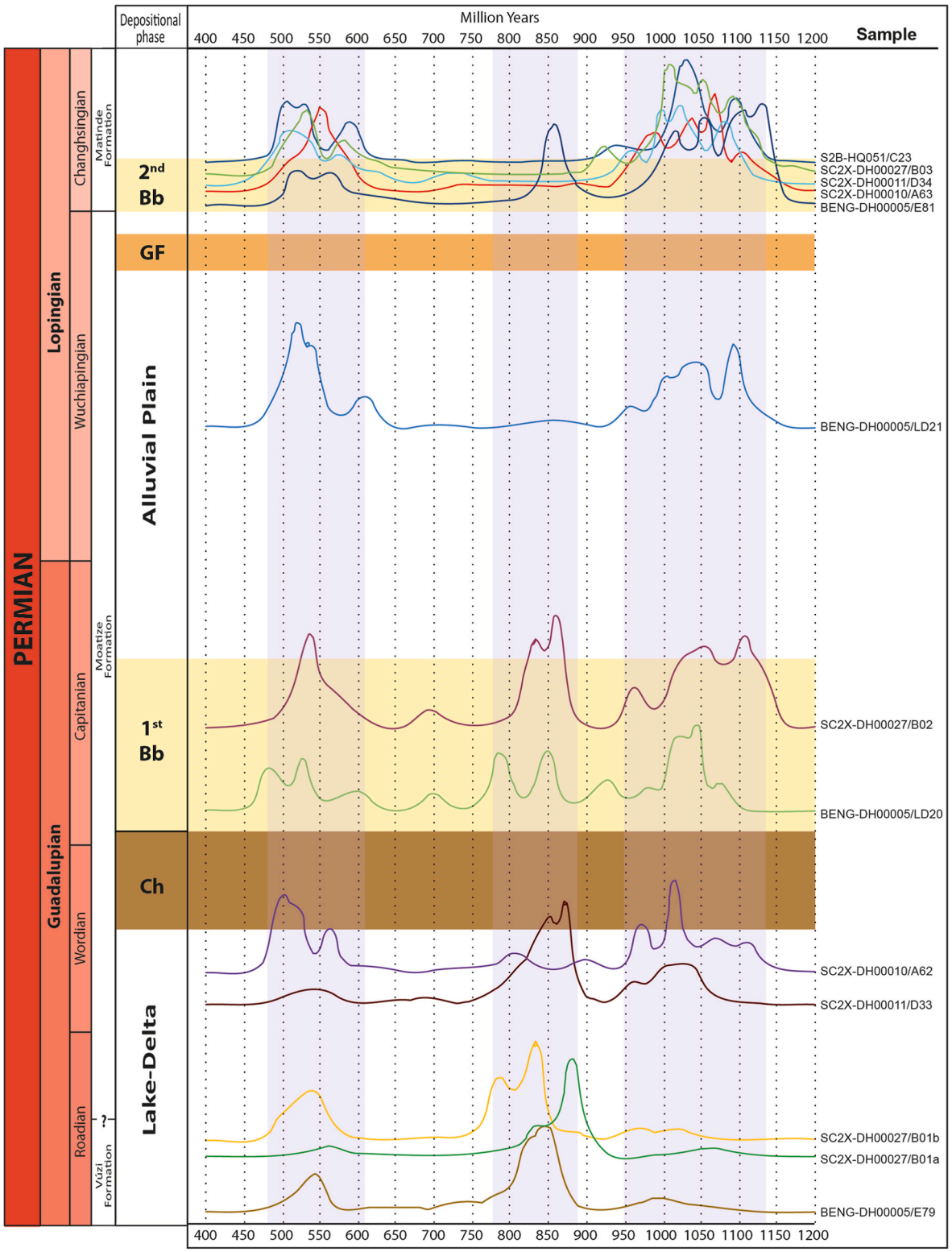

Fig. 6. Normalised probability density plots for the Moatize Coalfield U-Pb detrital zircon samples. The stratigraphic position of the samples is determined based on their age and depositional environments, as described by Fernandes et al. (2023).

the Vúzi and Moatize formations in the lake delta depositional phase, as well as in samples from the older (first) braided channel belt.

4.2. N'Condédzi Coalfield (Fig. 7, Table 2)

4.2.1. Alluvial plain depositional phase, Moatize Formation (above the ? Chipanga Seam, first braided channel belt)

In the N'Condédzi Coalfield, the oldest analysed sandstone samples are from the late Capitanian Moatize Formation and are tentatively

correlated with the underlying first braided channel belt (sample A1TM-058/LD58) and above the Chipanga Seam (sample A1TM-058/LD2) (Tables 1 and 2 and Fig. 5). These two samples are dominated by a unimodal Mesoproterozoic age population at 1094–989 Ma, with main peaks at 1036 and 1046 Ma.

4.2.2. Alluvial plain depositional phase, Matinde Formation (above the Grande Falésia seam, second braided channel belt)

Sample A1TM-058/LD22 is a sandstone interpreted as part of the second braided channel belt at the top of the Grande Falésia Seam. The U-Pb zircon age population clusters at 1091–988 Ma, with a main peak at 1027 Ma and a minor peak at 1084 Ma. 88% of the zircons are Mesoproterozoic and 11% Neoproterozoic. Samples A1TM-058/LD60 and A1TM-058/LD3 are sandstone beds interpreted as the channel-fill deposits of meandering rivers. They are dominated by a Mesoproterozoic unimodal U-Pb zircon population, similar to the previous samples. Sample A1TM-058/LD60 has a population at 1080–998 Ma with two peaks at 1034 Ma and 1046 Ma. In sample A1TM-058/LD3 the U-Pb zircon ages range from 1093 to 930 Ma, with a main peak at 1037 Ma. Sample CIMT-014/LD14 represents the last sandstone bed deposited before the Permo-Triassic Boundary. The detrital zircon U-Pb ages are similar to those found in the other Matinde Formation samples from borehole A1TM-58, with a main population at 1082–999 Ma and a prominent peak at 1043 Ma.

4.2.3. Alluvial plain depositional phase, Cádzi Formation – Lower Triassic

Five sandstone samples from the Lower Triassic Cádzi Formation (LD11, LD19, LD16, LD12, LD15, and LD17) were analysed in borehole CIMT-014. Samples LD11, LD15, LD16, and LD19 are coarse-grained sandstones and conglomerates representing channel-fills of braided rivers. They yield a zircon subpopulation between ca. 650–500 Ma, which is distinct from the age spectra of the upper Permian Moatize and Matinde formations.

The first sample above the Permo-Triassic Boundary, CIMT-014/LD11, yields a main zircon population from 1085 to 960, with a main peak at 1025 Ma and two minor peaks at 960 Ma and 1085 Ma. Other sub-populations are present at 952–930 Ma, 859–648 Ma and 618–519 Ma, with peaks at 598 Ma and 563 Ma. In this sample, 52% of the zircons are Mesoproterozoic (Stenian), followed by Neoproterozoic (24% Tonian and 13% Ediacran) and minor Paleoproterozoic and Paleozoic ages.

In sample CIMT-014/LD19, most of the U-Pb zircon population clusters at 1099–1008 Ma, with two prominent peaks at 1028 and 1042 Ma, with 92% of grains of Mesoproterozoic (Stenian) age. The remaining 8% of grains yield ages at 994–912 Ma, 820 Ma, 662 Ma and 544–535 Ma. Sample CIMT-014/LD16 is similar, with a primary population at 1085–948 Ma (peak at ca. 1035 Ma) and minor peaks at 1072 Ma, 1022 Ma and 988 Ma. Subpopulations are also present at 1776–1101 Ma, 948–846 Ma and 621–489 Ma, with peaks at 1110 Ma, 846 Ma and 589 Ma, respectively.

Sample CIMT-014/LD12 has 93% of zircons of Mesoproterozoic (Stenian) age and displays a clearly defined population at 1083–980 Ma (main peak at 1041 Ma and a smaller peak at 1027 Ma). Outside this age population, there is only a discrete peak at ca. 1106 Ma.

U-Pb zircon ages obtained from sample CIMT-014/LD15 reveal the presence of three distinct subpopulations. The primary subpopulation is 666–586 Ma, with 609 Ma and 627 Ma peaks. The second subpopulation is 541–489 Ma, with a peak at ca. 515 Ma. The third subpopulation displays a wide spectrum of ages ranging from 1131 to 932 Ma, with peaks at 1125 Ma, 1032 Ma and 1013 Ma.

Sample CIMT-014/LD17 displays a unimodal population at 1082–1009 Ma, with a main peak at 1040 Ma. 98 % of detrital zircons are of Mesoproterozoic age, and the remaining 2% are of Neoproterozoic age.

4.2.4. Alluvial plain depositional phase, Cádzi Formation – Upper Triassic

Upper Triassic sandstones were sampled in borehole CIMT-014 (sample LD13), and borehole A1TM-039 (samples LD9 and LD10). These samples are dominated by a unimodal U-Pb zircon age population ranging from 1090 to 898 Ma, with peaks at 1034 Ma, 1030 Ma and 1025 Ma.

5. Discussion

5.1. Summary of the detrital zircon U-Pb age spectra

In the Moatize Coalfield, the detrital zircon U-Pb ages can be grouped into three subpopulations at 1150–950 Ma, 900–780 Ma and 610–490 Ma. Only the 610–490 Ma subpopulation is found in all samples (including the different depositional facies and the three lithostratigraphic formations of the Moatize Coalfield) though in varying proportions (Fig. 6).

The 900–780 Ma subpopulation is observed in the lake delta depositional phase of the Vúzi (BENG-DH00005/E79, SC2X-DH00027/B01A and SC2X-DH00027/B01B) and Moatize formations (SC2X-DH00011/D33, SC2X-DH00010/A62). It is also seen in samples related to the first braided channel belt of the alluvial plain depositional phase in the Moatize Formation (BENG-DH00005-LD20 and SC2X-DH00027/B02) and in sample BENG-DH00005-E81 of the Matinde Formation related to the second braided channel belt. The deposition of these braided channel belts is associated with regional tectonic pulses that caused uplift in the watershed (Fernandes et al., 2023). To summarise, in the Moatize Coalfield, the zircon grains ranging from 900 to 780 Ma are associated with the sandstones of the Vúzi Formation deposited in a lake delta depositional setting and with sandstones of the Moatize and Matinde formations, deposited by bedload rivers in alluvial plain settings. Detrital zircons in this age range are not present in the N'Condédzi Coalfield.

In the sandstone samples in the Moatize Coalfield at the base of the Chipanga Seam, (samples SC2X-DH00011/D33 and SC2X-DH00010/A62), a zircon subpopulation at 1150–950 Ma is present. Interestingly, this subpopulation is also prominent in all other sandstone samples from the Moatize and Matinde formations. Based on the available data, it appears that the 1150–950 Ma source only becomes significant after the Chipanga Seam and was thus minor during the deglacial Lake delta deposition phase (Vúzi Formation).

The majority of zircon grains found in the N'Condédzi Coalfield have U-Pb ages between 1100 and 1000 Ma, with a peak at ca. 1040 Ma. There was, therefore, a relatively constant sediment supply from regions dominated by igneous rocks with U-Pb crystallisation ages between 1100 and 1000 Ma in the Moatize, Matinde, and Cádzi formations. There is a less significant zircon subpopulation at 610–490 Ma, with minor peaks at ca. 520, 610 and 630 Ma. However, the 610–490 Ma subpopulation only occurs in Lower Triassic age sandstones and is generally minor, with the exception of sample CIMT-014/LD15, where the 610–490 Ma subpopulation is predominant. The lower Triassic sandstones which yielded the 610–490 Ma subpopulation are coarse-grained amalgamated sandstone beds interpreted as channel-fill sequences of braided river channel belts that most likely formed during regional tectonic pulses. This population is not seen in the Upper Triassic, possibly due to regional tectonic activity. No zircon grains younger than 489 Ma and older than 1545 Ma were found in the N'Condédzi Coalfield sandstones.

When comparing the U-Pb ages of the zircon populations of the two coalfields, it is clear that the 900–780 Ma subpopulation is absent in the N'Condédzi Coalfield. The other two subpopulations, 610–490 Ma and 1150–950 Ma, are present in both coalfields, although 610–490 Ma zircons are rare in the N'Condédzi Coalfield. In particular, the upper part of the Moatize and the Matinde formations are coeval in both coalfields, but these formations differ significantly in their zircon populations. The only zircon subpopulation common to both formations ranges is

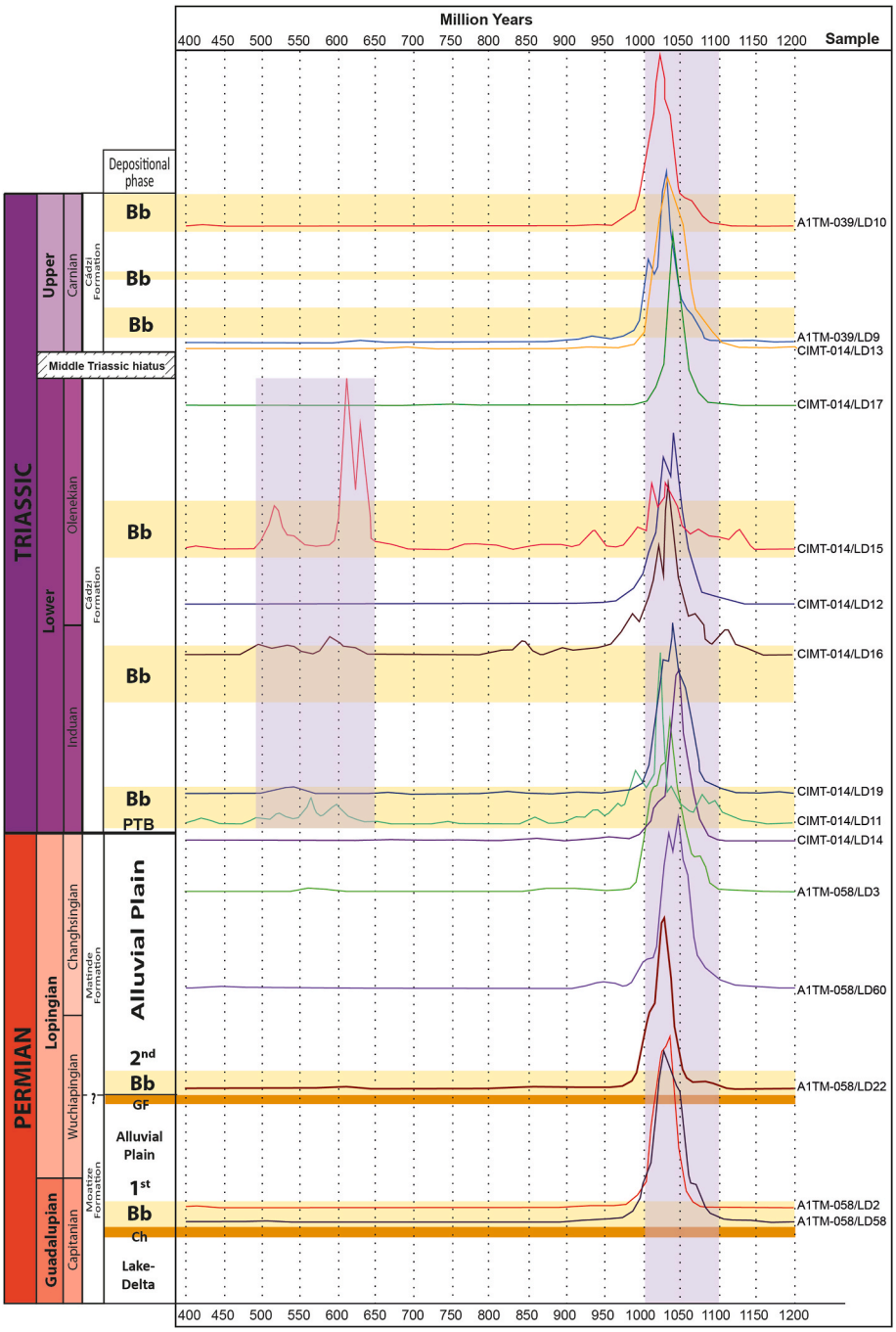

Fig. 7. Normalised probability density plots for the N'Condédzi Coalfield U-Pb detrital zircon samples. The stratigraphic position of the samples is determined based on their age and their depositional environment, as described by Galasso et al. (2019b).

1150–950 Ma, which is prominent in the N'Condédzi Coalfield. This suggests that the two coalfields had different sediment sources, indicating they were not fully connected during the deposition of the two coal-bearing formations.

The sandstones of the Cádzi Formation were only sampled in the N'Condédzi Coalfield. All the sandstones of the last formation have a main zircon subpopulation between 1100 and 1000 Ma. However, a minor subpopulation, at 650–490 Ma, is present only in the Lower Triassic samples. This suggests that during the deposition of the Cádzi Formation, despite the Middle Triassic hiatus detected by the palynomorph ages, the main sedimentary source areas remained constant, with terranes exposing rocks within the 1100–1000 Ma age interval. Only during Lower Triassic times were terranes within the 650–490 Ma age interval available as sediment sources for the N'Condédzi Coalfield. Nonetheless, during the deposition of the Cádzi Formation, rock units within the 900–780 Ma age interval were never exposed to erosion in the source areas of this basin.

5.2. Detrital zircon provenance analysis

5.2.1. Regional sources

The Moatize and N'Condédzi coalfields are surrounded by cratons and mobile belts ranging in age from Archaean to early Palaeozoic (Figs. 1 and 2). To the south and east of these coalfields, the geology consists of the Zimbabwe Craton, part of the great Kalahari Craton and surrounding Proterozoic to early Palaeozoic mobile belts, namely the

Table 2
Summary of the detrital zircon U–Pb LA-ICP-MS data for the Moatize Coalfield. Arch – Archaean, Paleoprot – Palaeoproterozoic, Mesoprot – Mesoproterozoic, Neoprot – Neoproterozoic, Ton – Tonian, Cry – Cryogenian, Edi – Ediacaran, Cam – Cambrian, Ord – Ordovician, Sil – Silurian, Dev – Devonian, Carb – Carboniferous.

Moatize Coalfield																					
Borehole	Samp. ref.	Format.	Deposit. phase	# Grains	Youngest zircon (Ma)	Oldest Zircon (Ma)	Populations (Ma)	Peaks (Ma)			Age distribution (%)										
								1st	2nd	3rd	Palaeozoic					Neoprot			Meso prot	Paleo prot	Arch
											Carb	Dev	Sil	Ord	Cam	Edi	Cry	Ton			
BENG-DH00005	E81	Matinde	Alluvial Plain	120	486	1166	512-519; 531–540; 556–576; 591; 615–629; 689; 734; 750; 807–810; 836–899; 923; 938; 957–960; 979–1145; 1166	1130	850; 1011; 1053	514; 558					6.7	9.2	0.8	27.5	55.8		
	LD21	Moatize	Alluvial Plain	120	406	1362	469; 481–578; 599-624; 691; 729; 823–830; 867–871; 883; 949–962; 976; 989–1011; 1025-1068; 1081–1139; 1362	517; 1091	1043	605		0.8		1.7	24.2	15.8	0.8	13.3	43.3		
	LD20	Moatize	Alluvial Plain	56	475	2699	477; 480; 490; 499; 507; 525–532; 555; 579; 597607; 695–702; 760; 780–800; 825; 838–862; 894; 913; 926–941; 973; 981; 995; 1010–1048; 1070-1083; 2657; 2699	1040	477; 526; 785; 841	598; 700; 928				5.4	12.5	7.1	3.6	39.3	28.6		3.6
	E79	Vúzi	Lake Delta	142	481	1587	487-489; 506; 513–559; 573; 603; 616; 649–652; 670; 685; 719–727; 738; 750–752; 766; 780–791; 802-887; 923; 936; 967–979; 989-1017; 1035–1066; 1587	844	540	729; 992				0.7	9.9	9.9	4.9	60.2	8.5		
SC2X-DH00027	B03	Moatize	Alluvial Plain	107	344	1700	500-549; 568–584; 611-617; 636; 6601; 710; 738; 915–929; 949; 966; 971–1126; 1157; 1194; 1700	1007	533; 1061; 1095	590; 920											
	B02	Moatize	Alluvial Plain	88	327	1237	467; 502–577; 596-598; 689–690; 711; 775; 812–880; 956-981; 1000–1143; 1237	534; 860	1064; 1104	960	1.1			1.1	10.2	10.2	4.5	30.7	42.0		
	B01B	Vúzi	Lake Delta	110	494	2587	494-502; 514–556; 568-569; 586; 598; 667–671; 707; 743; 758–887; 928; 959–973; 1009-1036; 2587	830	636; 785	960; 1020					17.3	11.8	2.7	61.8	5.5		0.9
	B01A	Vúzi	Lake Delta	115	496	2676	534; 546–549; 558-566; 582–595; 638; 685; 700; 712; 725; 754–758; 794-799; 822–920; 1008; 1024; 1037–1048; 1063-1095; 2682-2676	882	558						1.7	7.8	3.5	75.7	9.6		1.7
SC2X-DH00010	A63	Matinde	Alluvial Plain	123	482	1586	482-485; 499–587; 602-603; 635; 732; 745; 769; 801–806; 837; 878; 898–900; 950-1080; 1098–1146; 1198; 1586	545; 1068	986; 1035	730; 870				1.6	8.9	22.0		22.8	44.7		
	A62	Moatize	Lake Delta	104	478	1735	487-542; 559–576; 600; 614; 623; 730; 754–757; 795-826; 841; 879; 894–908; 928; 954; 967–991; 1004-1129; 1167; 1653; 1735	500; 1015	560; 969; 1067	804				1.0	24.0	11.5		25.0	36.5	1.9	
SC2X-DH00011	D34	Matinde	Alluvial Plain	116	464	1690	464-466; 478–482; 495-598; 621–622; 650; 696; 718; 737–751; 799-804; 855; 879; 901; 912; 938–1109; 1137-1139; 1690	1021	509; 1083	574; 949				4.3	14.7	14.7	3.4	22.4	39.7	0.9	
	D33	Moatize	Lake Delta	108	498	1073	498-509; 529–548; 559-565; 640–645; 687; 698; 762–770; 786-889; 901; 929; 959–1048; 1065-1073	871	1034	553					4.6	4.6	4.6	67.6	18.5		
S2B-HQ051	C23	Matinde	Alluvial Plain	124	465	1721	470; 494–539; 563-603; 635–640; 727; 833; 907; 932–946; 962-963; 979–1068; 1085-1130; 1194; 1721	1031	501; 586; 1093	930				1.6	21.0	12.1	0.8	10.5	54.0		

Table 3
Summary of the detrital zircon U–Pb LA-ICP-MS data for the N'Condédzi Coalfield. Arch – Archaean, Paleoprot – Palaeoproterozoic, Mesoprot – Mesoproterozoic, Neoprot – Neoproterozoic, Ton – Tonian, Cry – Cryogenian, Edi – Ediacaran, Cam – Cambrian, Ord – Ordovician, Sil – Silurian, Dev – Devonian, Carb – Carboniferous.

N'Condédzi Coalfield																				
Borehole	Samp. ref.	Format.	Deposit. phase	No Grains	Youngest zircon (Ma)	Oldest Zircon (Ma)	Populations(Ma)	Peaks (Ma)			Age distribution (%)									
								1st	2nd	3rd	Palaeozoic					Neoprot			Meso prot	Paleo prot	Arch
											Carb	Dev	Sil	Ord	Cam	Edi	Cry	Ton			
A1TM-058	LD3	Matinde	Alluvial Plain	121	880	1093	980; 998-1093	1037	1027; 1014	1075						2.0		6.0	92.0		
	LD60	Matinde	Alluvial Plain	123	946	1108	994; 998–1080; 1087–1094; 1108	1046	1034	1003; 950			1.0					6.0	93.0		
	LD22	Matinde	Alluvial Plain	122	968	1091	988-1065; 1083-1091	1027	1084							1.0		11.0	88.0		
	LD2	Moatize	Lake Delta	120	942	1060	994–1060	1036				1.0						6.0	93.0		
	LD58	Moatize	Lake Delta	119	506	1545	915; 952; 989–1080; 1093; 1545	1029	1074						1.0			6.0	92.0		
CIMT-014	LD13	Cádzi	Alluvial Plain	121	930	1181	993-1091; 1114; 1181	1025	1063								1.0	2.0	97.0		
	LD17	Cádzi	Alluvial Plain	120	706	1099	1009-1082; 1099	1040									1.0	1.0	98.0		
	LD15	Cádzi	Alluvial Plain	119	502	1131	502-531; 539–541; 586; 599–643; 654; 666; 765; 778; 856; 873; 896; 923–941; 974; 989–1063; 1072-1076; 1088–1091; 1103-1105; 1122-1131	609; 627	515	1013; 1032; 1125			1.0		9.0	38.0	5.0	13.0	34.0		
	LD12	Cádzi	Alluvial Plain	120	974	1106	980-989; 998–1068; 1076-1083; 1106	1041	1027	1106								7.0	93.0		
	LD16	Cádzi	Alluvial Plain	120	489	1776	489-492; 501; 516; 528542; 579; 588–600; 615-621; 846–848; 948-1085; 1091; 1101–1118; 1133-1137; 1776	1035	988; 1022; 1072	589; 846; 1110					5.0	6.0		20.0	69.0		
	LD19	Cádzi	Alluvial Plain	121	522	1099	535-544; 662; 820; 912; 994; 1008-1099	1028; 1042							2.0	1.0	1.0	4.0	92.0		
	LD11	Cádzi	Alluvial Plain	118	492	1710	519-526; 540; 560–567; 577; 585–603; 612-618; 648; 743; 859; 930–941; 951; 960–1085; 1094-1122; 1143; 1710	1025	960; 1085	563; 598	2.0	2.0	1.0		4.0	13.0	1.0	24.0	52.0	1.0	
	LD14	Matinde	Alluvial Plain	122	943	1082	980; 999-1082	1043	1019								1.0	6.0	93.0		
A1TM-039	LD10	Cádzi	Alluvial Plain	120	981	1090	985-1068; 1076; 1090	1025	1030	1034		1.0						9.0	90.0		
	LD9	Cádzi	Alluvial Plain	119	898	1145	932; 946; 977–985; 993-1076; 1116; 1145									1.0		10.0	89.0		

Zambezi, Choma-Kaloma, Nampula and Báruè Blocks, and the Magondi Belt (Goscombe et al., 2020; Hanson, 2003). To the northeast, the coalfields are bordered by Meso-Neoproterozoic mobile belts including the Southern Irumide Belt, the Irumide Belt, the Kibaran Belt, the Cabo Delgado Nappe Complex and the Lufilian Arc (Bingen et al., 2009; Chaúque et al., 2019; Hanson, 2003; Johnson et al., 2006; Macey et al., 2010). The oldest terranes to the north comprise the Palaeoproterozoic Bangweulu Block and the Palaeoproterozoic (2200 Ma to 1800 Ma) Ubendian - Usagaran Belts. The wide ranges in age of these diverse sources thus represent an ideal opportunity to constrain the provenance of the Moatize and N'Condédzi coalfields.

As most of the zircon grains populations have ages ranging from 1150 to 450 Ma, this indicates that the source terranes for both Karoo depocenters were the Mesoproterozoic Grenvillian orogenic belts (1350–1000 Ma) nearby, which include the Kibaran, Irumide, and Southern Irumide belts, as well as the Choma-Kaloma, Nampula, and Báruè Blocks, and the Pan-African orogenic belts (650–450 Ma), comprising the Zambezi Belt, the Cabo Delgado Nappe Complex, Lúrio Belt and the Lufilian Arc (Fig. 1). These units are discussed below. Archaean cratons (>2500 Ma) and the Paleoproterozoic mobile belts (2200–1800 Ma) are unlikely to be the primary source terrains for these Karoo depocenters due to the very minor amounts of zircon grains of these ages.

5.2.2. Source terranes for the 650–490 Ma zircon subpopulation (Figs. 2 and 8)

The zircon subpopulation within the age range of 650–490 Ma is most likely associated with Pan-African granitoids present in the Lúrio Belt, Nampula Block, and the Southern Irumide Belt (Fig. 2). These intrusions include the Malema Suite, dated from 532 to 502 Ma, and the Murrupula Suite, dated from 535 to 495 Ma, in the Nampula Block and Lúrio Belt. Pan-African granites and syenites ranging from 543 to 474 Ma are also found in the Southern Irumide terranes of Zambia, and South Malawi and the Western Niassa province of Mozambique where crystallisation ages range from 562 to 515 Ma.

In the Cabo Delgado Nappe Complex (Fig. 2), intrusive granitoids and orthogneiss are within the age range of 650–490 Ma. These rocks were thrust over the Southern Irumide Belt and have crystallisation ages ranging from 799 to 591 Ma (Jamal, 2005; Norconsult Consortium, 2007). The Monapo Complex also contains intrusive rocks that were emplaced in the same nappe complex, and have U/Pb zircon ages ranging from 637 to 635 Ma (Grantham et al., 2007; Jamal, 2005).

5.2.3. Source terranes for the 900–780 Ma zircon subpopulation (Figs. 2 and 8)

In western Zambia, the Late Mesoproterozoic (1106–1090 Ma) basement rocks of the Zambezi Belt (Hanson et al., 1988; Katongo et al., 2004) are unconformably overlain by supracrustal sequences comprising metavolcanic rocks that yielded crystallisation ages ranging from ca. 880 Ma (Kafue Rhyolite) (Johnson et al., 2007) to ca. 795 Ma (Chironga Gneiss) (Hargrove et al., 2003). Portions of the supracrustal sequences are intruded by the 820 Ma Lusaka Granite (Johnson et al., 2007). The Zambezi Allochthonous Terrane is found in the eastern part of the Zambezi Belt along the Zimbabwe-Mozambique border. It is characterised by thick-skinned tectonics and an inverted crustal column (Hargrove et al., 2003). The Zambezi Allochthonous Terrain was thrust over the Neoproterozoic supracrustal Rushinga Metamorphic Suite, which includes the ca. 795 Ma Chironga Gneiss. The Zambezi Allochthonous Terrain consists of two thrust slices, the orthogneisses of the Masoso Suite and the Mavuradonha Metagabbroic Complex. Gneisses of the Masoso Suite yield zircon U-Pb crystallisation ages of the protoliths from 1051 to 850 Ma (Mariga et al., 1998; Vinyu et al., 1999). The basal Rushinga Igneous Complex intrusive rocks have yielded a U-Pb zircon crystallisation age of 805 Ma.

In Mozambique, the outcrops of the Zambezi Allochthous Terrane are limited in extent and geochronological data. The most representative units of the Zambezi Belt in Mozambique are the Rushinga Group and the Guro Suite. The Rushinga Group comprises metasediments and the Guro Suite is made of metamorphosed granitoids (charnockites, granite-gneisses, and TTG) (GTK Consortium, 2006a; Manjate and Tassinari, 2018). The granitoids of the Guro Suite have yielded zircon U-Pb crystallisation ages of 867 Ma and 852 Ma (Mäntäri, 2008) and 835 Ma, 824 Ma and 822 Ma (Manjate and Tassinari, 2018), all within the 900–780 Ma age range.

The Ocua Complex is a tectonic mélange located in the core of the Lúrio Belt, and consists of metasediments, granulites, and gneisses that can be traced from adjacent geological units of the Nampula Block and Southern Irumide Belt (Grantham et al., 2011) (Fig. 2). The Ocua Complex Group metasediments have yielded detrital zircon ages between 978 – 922 Ma and 880–768 Ma (Jamal, 2005; Norconsult Consortium, 2007). The Lúrio Belt is intruded by the late Pan-African granitoids of the Malema Suite dated from 532 to 502 Ma (Bingen et al., 2009; Norconsult Consortium, 2007).

Few magmatic rocks within the 900–780 age interval are found in the other mobile belts that encircle the two coalfields. Such rocks are mostly found in the Southern Irumide Belt in southern Malawi, western Tete province and the western Niassa province in Mozambique. These rocks comprise a small group of syenites and mafic intrusions that were emplaced between 808 and 600 Ma, including the 729 Ma nepheline-bearing gneiss in southern Malawi (Ashwal et al., 2007), the 788 Ma Monte Chissindo syenite in Niassa province (Norconsult Consortium, 2007), and the 864 ± 30 Ma mafic rocks of the Atchiza Suite (Mäntäri, 2008).

Detrital zircon grains within the 900–780 Ma age range are also found in metasedimentary sequences, but always as minor subpopulations, in the Nampula Block and Báruè Complex. Given the paucity of Archaean and Palaeoproterozoic zircons in the studied Karoo successions, we disregard any metasedimentary sequences that also contain significant proportions of Archaean and Palaeoproterozoic detritus. These metasedimentary include the strongly deformed meta-psammites and meta-conglomerates of Mecubúri and the Alto Benfica Groups (Thomas et al., 2010) that unconformably overlie the Mesoproterozoic rocks of the Nampula Block (Norconsult Consortium, 2007) (Fig. 2), and the metasedimentary Chimoio and Macossa Groups of the Báruè Complex (Chaúque et al., 2019; Grantham et al., 2011; GTK Consortium, 2006a). The Zambezi Belt is, therefore, the most likely source of the detrital zircon grains found in the Moatize Coalfield in the 900–780 Ma age range.

5.2.4. Source terranes for the 1150–950 Ma zircon subpopulation (Figs. 2 and 8)

Zircon grains within the age range of 1150 to 950 Ma are the most common among all subpopulations. A large number of terranes of this age are located in the mobile belts adjacent to the Moatize and N'Condédzi coalfields.

The basement rocks of the Zambezi Belt in eastern Zambia and northern Zimbabwe comprise Late Mesoproterozoic orthogneisses, including the ca. 1106 Ma Mpande Gneiss (Hanson et al., 1988) and the ca. 1090 Ma Munali Hill Granite (Katongo et al., 2004). The ocellar gneisses of the Masoso Suite in the Zambezi Allochthonous Terrane have yielded zircon U-Pb zircon crystallisation ages of the protoliths between 1051 and 870 Ma (Hargrove et al., 2003).

The Nampula Block (Fig. 2), located east of the Moatize and N'Condédzi coalfields, comprises mainly Mesoproterozoic rocks deformed at ca. 1000 Ma. The WSW-ENE trending Lúrio Belt separates the Nampula Block from the Southern Irumide Belt. The Lúrio Belt is a structure formed during the folding of the Cabo Delgado Nappe Complex, later reactivated as a shear zone (Viola et al., 2008). The Mocuba Suite is the oldest unit in the Nampula Block and comprises metasedimentary and metavolcanic sequences, with intrusive trondhjemite-tonalite-granite orthogneiss suites that formed in a magmatic arc (Bingen et al., 2009; Kröner et al., 1997; Macey et al.,

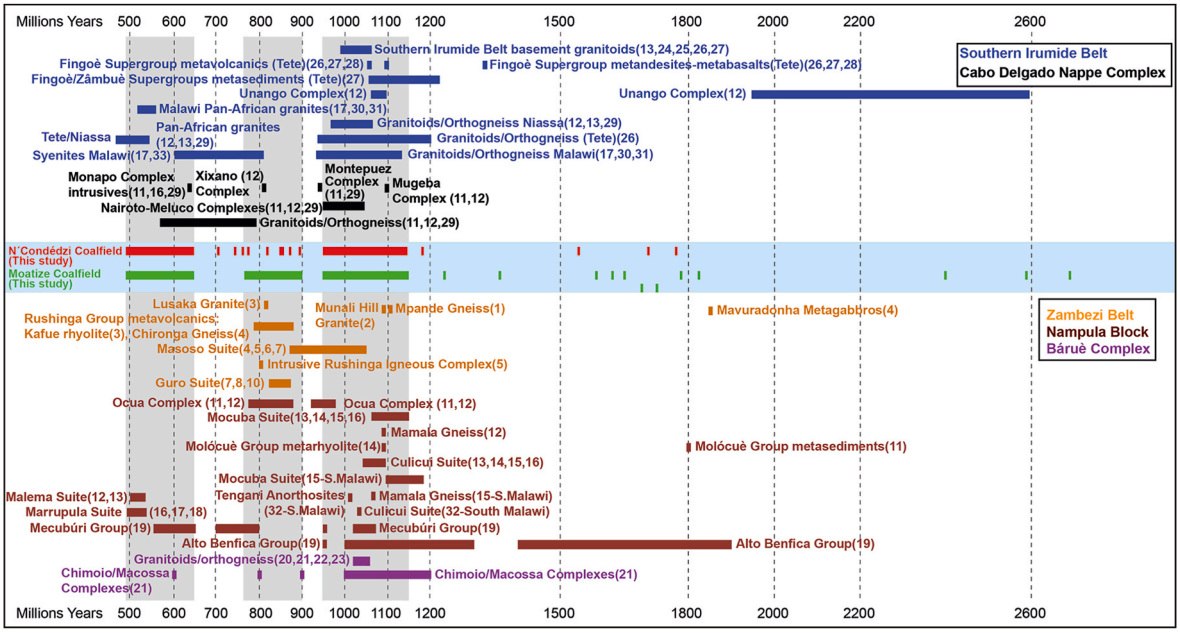

Fig. 8. Major tectonomagmatic events and zircon ages of the several geologic units in the Southern Irumide Belt, Cabo Delgado Nappe Complex, Zambezi Belt, Nampula Block and Báruè Complex. The vertical pale-grey bars indicate 650–490 Ma, 900–780 Ma and 1150–950 Ma time windows. Data sources are: (1) Hanson et al. (1988), (2) Katongo et al. (2004), (3) Johnson et al. (2007), (4) Hargrove et al. (2003), (5) Sakuwaha et al. (2022), (6) Mariga et al. (1998), (7) Vinyu et al. (1999), (8) GTK-Consortium, 2006, (9) Mäntäri (2008), (10) Manjate and Tassinari (2018), (11) Jamal (2005), (12) Norconsult-Consortium (2007), (13) Bingen et al. (2009), (14) Macey et al. (2010), (15) Kröner et al. (1997), (16) Macey et al. (2007), (17) Thomas et al. (2022), (18) Grantham et al. (2007), (19) Grantham et al. (2008), (20) Jacobs et al. (2008), (21) Thomas et al. (2010), (22) Chaúque (2012), (23) Chaúque et al. (2019), (24) Manjate (2012), (25) Manjate (2015), (26) Westerhof et al. (2008), (27) Petry et al. (2022), (28) Kröner et al. (2001), (29) Manda et al. (2019), (30) Tsunogae et al. (2021), (31) Ashwal et al. (2007), (32) Thomas et al. (2022).

2007, 2010; Manhiça et al., 2001). The orthogneisses yield protolith ages ranging from 1148 to 1063 Ma (Macey et al., 2010), whereas an age of 1092 Ma was obtained from the Mamala Gneiss, a metavolcanic rock within the Mocuba Suite (Macey et al., 2007). The rocks of the Mocuba Suit are covered by the Molócuè Group, consisting of paragneiss and metavolcanic rocks. Metarhyolites of the Molócuè Group have yielded crystallisation ages of 1092–1090 Ma. Detrital zircons from the Molócuè Group yield a main age peak at ca. 1100 Ma and a subpopulation at 1800 Ma (Macey et al., 2010). The youngest concordant detrital zircon is 1115 ± 19 Ma, which can be regarded as the maximum deposition age. All the units above are intruded by the orthogneisses of the Culicui Suite, the most voluminous and widespread unit in the Nampula Block (Macey et al., 2010). The orthogneisses of the Culicui Suite have yielded zircon protoliths ages ranging from 1094 to 1042 Ma (Bingen et al., 2009; Kröner et al., 1997; Macey et al., 2007, 2010).

The major rock units of the Nampula Block were recognised by Thomas et al. (2022) in south Malawi (Malawi Complex, Fig. 2), with zircon ages similar to the units defined in Mozambique. Orthogneisses of the Mocuba suite yield U-Pb zircon ages ranging from 1180 to 1094 Ma, the Mamala Gneiss at 1065 Ma, and the Culicui Suite yields an age of 1043 Ma. The Molócuè Group does not outcrop in south Malawi. The post-tectonic Tengani Suite anorthosites have yielded an emplacement age of 1008 Ma (Thomas et al., 2022).

The Báruè Complex borders the Zimbabwe Craton to the west and the Zambezi Belt to the north. To the east is covered by sedimentary rocks and sediments, ranging in age from the Jurassic to recent. It consists of a crystalline basement of granitoid-orthogneisses, overlain by two groups of metasedimentary rocks, the Chimoio and Macossa Groups (Chaúque et al., 2019; Grantham et al., 2011; GTK Consortium, 2006a). Several granitoid–orthogneisses bodies yield U-Pb zircon crystallisation ages ranging from 1156 to 1016 Ma (Chaúque, 2012; Chaúque et al., 2019; Manjate, 2012, 2015).

The Southern Irumide Belt (Fig. 2) trends WSW-ENE and can be traced from Zambia to NW Zimbabwe, Mozambique (Tete province), central and south Malawi and NE Mozambique (Niassa and Cabo Delgado provinces). To the south, the Southern Irumide Belt is separated from the Zambezi Belt and Nampula Block by the Sanângoè Shear Zone and Lúrio Belt, respectively, while to the east, it is in contact with the Neoproterozoic Cabo Delgado Nappe Complex of the Mozambique Belt. The Southern Irumide Belt comprises a late Palaeoproterozoic(?) to late Mesoproterozoic crystalline basement composed of metasedimentary and metavolcanic suites (Johnson et al., 2005; Westerhof et al., 2008). This basement has been intruded by granitoids with emplacement ages ranging from ca. 1060–1000 Ma (Bingen et al., 2009; GTK Consortium, 2006a; Johnson et al., 2006; Mäntäri, 2008; Norconsult Consortium, 2007; Westerhof et al., 2008).

The age of the metasedimentary and metavolcanic sequences in the basement of the Southern Irumide Belt is not well constrained. Meta-andesites within the metasedimentary basement rocks of the Tete province, Mozambique (Fíngoè Supergroup) yield crystallisation ages of ca. 1327 Ma (Mäntäri, 2008), ca.1095 Ma (Petry et al., 2022), and a mafic gneiss interpreted as an original basaltic lava has yielded a crystallisation ages of ca. 1058 Ma (Council for Geoscience, 2007). Detrital zircon ages range from 2635 to 1052 Ma in the Tete province metasedimentary units, but with a near unimodal population at ca. 1200–1106 Ma and maximum deposition ages of between 1143 and 1077 Ma (Petry et al., 2022). In the Niassa province of NE Mozambique, detrital zircon ages from metasedimentary rocks within the Unango Complex (Fig. 2) range from 2596 to 1062 Ma with a maximum deposition age of 1062 Ma (Norconsult Consortium, 2007).

The crystalline basement of the Southern Irumide Belt is mainly composed of suites of granitoid-orthogneiss that intrude the metasedimentary units. In Mozambique, the crystallisation ages of these granitoid suites range between 1201 and 939 Ma in the Tete-Chipata terrane (Mäntäri, 2008) and in the Niassa province from 1065 to 968 Ma in the Unango and Marrupa complexes (Bingen et al., 2009; Jamal, 2005; Norconsult Consortium, 2007). In southeastern Zambia, three granitoid emplacement ages were recognised; the most voluminous ranges

between 1076 and 1008 Ma. Granitoid emplacement also took place at 2000–1950 Ma and 742–647 Ma (Johnson et al., 2006). In the Southern Irumide Belt in southern Malawi, basement granitoid-orthogneiss complexes have yielded zircon U-Pb crystallisation ages from 1130 to 929 Ma (Kröner et al., 2001; Manda et al., 2019; Tsunogae et al., 2021).

The Cabo Delgado Nappe Complex (Fig. 2) is a stack of Neoproterozoic nappes (the Muaquia, M'Sawize, Lalamo, Montepuez and Xixano complexes) thrust over the Mesoproterozoic terranes (the Unango, Marrupa, Nairoto and Meluco complexes) of the Southern Irumide Belt in Mozambique (Viola et al., 2008). Also included in the Cabo Delgado Nappe Complex are the Monapo and Mugeba complexes that were thrust over the Nampula Block (Fig. 2). The Nairoto and Meluco basement complexes have yielded protolith crystallisation ages ranging from 1044 to 944 Ma (Jamal, 2005; Norconsult Consortium, 2007). The oldest zircon ages from the stacked nappes come from a paragneiss leucosome within the Montepuez Complex dated at 942 Ma (Jamal, 2005) while a meta-rhyolite within the Xixano Complex has been dated at 818 Ma (Norconsult Consortium, 2007). In the nappes thrust over the Nampula Block, the Mugeba Complex has yielded a crystallisation age of ca. 1100 (Macey et al., 2007), while the intrusive

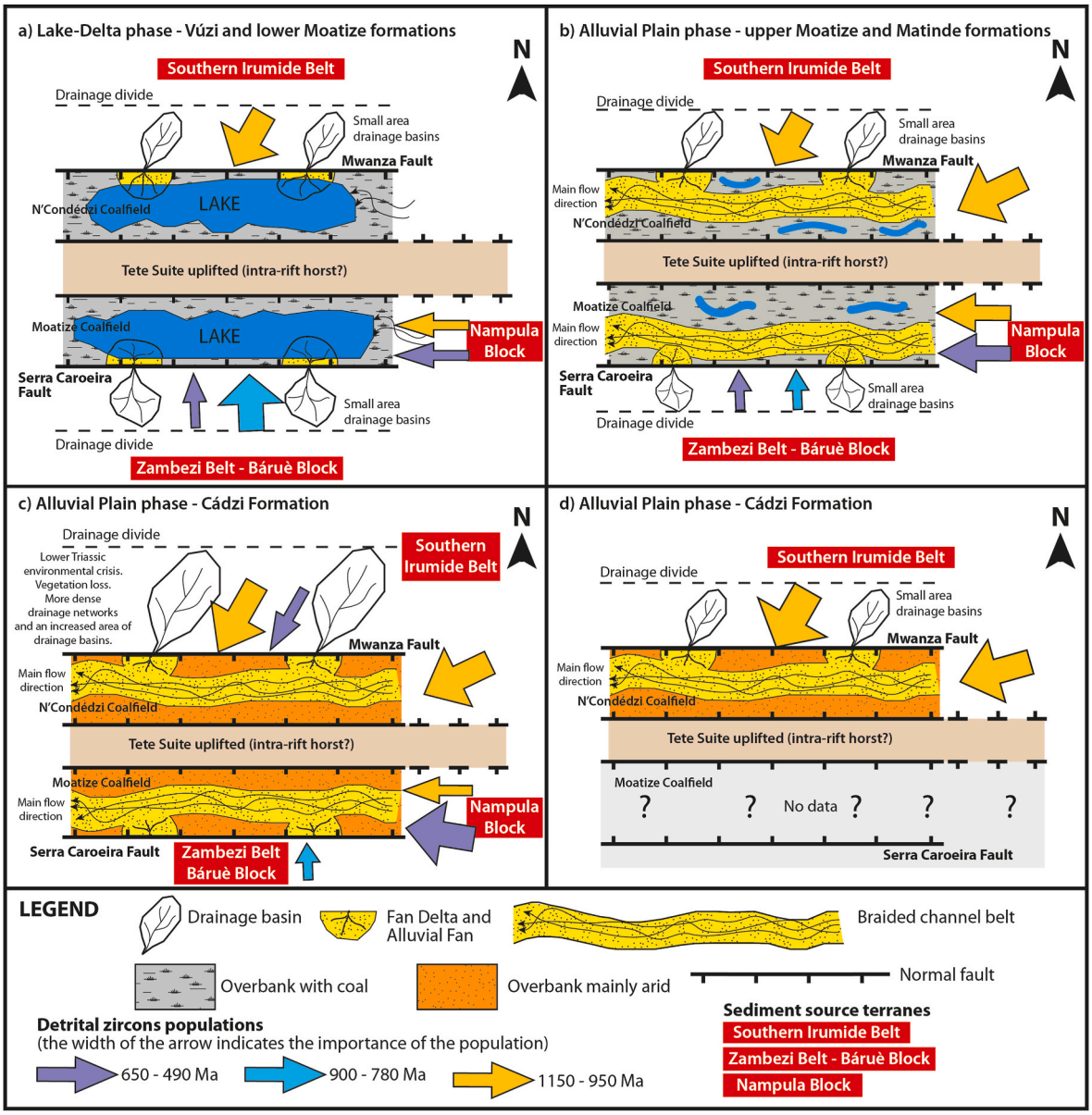

Fig. 9. Schematic diagrams illustrating the evolution of tectonosedimentary history of the Moatize and N'Condédzi coalfields. **(a)** Lake delta depositional phase corresponds to the Vúzi Formation and the lower part of the Moatize Formation (early Roadian to late Wordian). The pre-existing topography (Tete Suite) gave rise to an intra-rift horst, which physically separated the two coalfields and constrained the provenance and sediment routing system. The provenance areas were proximal and limited to the rift shoulders. **(b)** The alluvial plain depositional phase corresponds to the upper part of the Moatize Formation and all of the Matinde Formation (early Capitanian to late Changhsingian). During this phase, two significant tectonic events occurred, marked in the stratigraphy by two braided channel belts. During this phase, intra-rift horst remained a prominent geomorphologic feature, not allowing the connection of the two coalfields. **(c)** Alluvial Plain depositional phase corresponds to the lower part of the Cádzi Formation (Lower Triassic). The environmental and climatic disruptions at the end of the Permian period had a significant impact on terrestrial ecosystems, leading to a complete loss of vegetation in the rift basin and upland areas. This resulted in the formation of more dense drainage networks and an expansion of the drainage basin areas in the rift shoulders of the N'Condédzi Coalfield. The provenance interpretation for the Moatize Coalfield is after Bicca et al. (2017). **(d)** The alluvial plain depositional phase corresponds to the upper part of the Cádzi Formation (Upper Triassic). Note that figures (a)–(d) are not drawn to scale.

rocks in the Monapo Complex ranges in age from 637 to 635 Ma (Grantham et al., 2007; Jamal, 2005).

5.3. Sediment dispersal pathways and basin evolution (Fig. 9)

5.3.1. Lake delta depositional phase – early Roadian to late Wordian (Fig. 9a)

This depositional phase corresponds to the succession up to the Chipanga Seam and is represented by the Vúzi Formation and the lower part of the Moatize Formation. The Vúzi Formation was not identified in the N'Condédzi Coalfield, and therefore, discussion is limited here to the Moatize Coalfield. The dominant detrital zircon subpopulation in the Vúzi Formation is 900–780 Ma, followed by the 650–450 Ma subpopulation. The age distribution of the zircon population suggests that the predominant source is located in the Zambezi Belt (Fig. 2). This observation is consistent with the ages of the Guro Suite, Masoso Suite, and the metavolcanics that are present in the supracrustal Rushinga Group of the Zambezi Belt (Fig. 8).

Another possible sediment source for the Vúzi Formation could be the Ocua Complex (Mäntäri, 2008; Manjate and Tassinari, 2018) because its detrital zircon population matches the detrital zircon population in the Vúzi and lower Moatize formations. This would imply sediment transport from east to west. However, the Ocua Complex exposure is limited, and a source in this region would also likely include derivation of 1350–1000 Ma zircon from the Nampula Block and the Southern Irumide Belt of northwest Mozambique (the Unango and Marupa Complexes) and south Malawi (Malawi Complex). Zircons in the 1350–1000 Ma age range are not seen in the Vúzi Formation but are present in the lower part of the Moatize Formation below the Chipanga Seam. Hence the Ocua Complex could be a source for the Moatize Coalfield following deposition of the Vúzi Formation.

The Vúzi Formation in the Chicôa-Mecúcoè Sub-Basin (Borehole 11MTD001, Fig. 2) yielded detrital zircons with a dominant subpopulation at 1200–900 Ma with a peak at 1080 Ma (Whitecross, 2020). Additionally, there are minor peaks at 560–520 Ma and 780–697 Ma (Fig. 8) (Whitecross, 2020). These age spectra do not resemble those of the Vúzi Formation in this study, with the only common peak being the minor 560–520 Ma subpopulation. The Chicôa-Mecúcoè Sub-Basin lacks the 900–750 Ma age interval found in the Moatize Coalfield, while its main 1200–900 Ma is either absent or minor in the Vúzi Formation of the Moatize Coalfield. The Vúzi Formation in the Moatize Coalfield and the Chicôa-Mecúcoè Sub-Basin were therefore sourced from terranes of different age, the Chicôa-Mecúcoè Sub-Basin most likely from the Southern Irumide Belt located to the north or northeast (Whitecross, 2020) (Fig. 2), and the Moatize Coalfield from the Zambezi Belt to the south and (less likely) from the Lúrio Belt/Nampula Block to the east.

Noteworthy, in the Moatize Coalfield, a shift in the sediment provenance is detected in the samples of the lower part of the Moatize Formation, below the Chipanga Seam, with the subpopulation ranging from 1150 to 950 Ma starting to become prominent. This indicates a sediment source in the basement rocks of the Zambezi Belt, located in eastern Zambia and northern Zimbabwe and from the Nampula Block. However, several units of the Cabo Delgado Nappe Complex have zircon ages between 1150 and 950 Ma, and should not be dismissed as potential source areas if exposed during the initial phases of the Moatize Formation depositional cycle.

In conclusion, the lower part of the Moatize Formation formed during the final stages of the lake delta deposition phase, with sandstone beds deposited during this time interval associated with the development of the Chipanga Seam. The detrital zircon population of these beds points towards a source in the Zambezi Belt, specifically the Guro Suite and Báruè Complex. However, the first appearance of a 1150–950 Ma zircon subpopulation indicates derivation from the Nampula Block to the east and possibly from Southern Irumide Belt to the north-northeast.

In the study of Whitecross (2020) on the Chicôa-Mecúcoè Sub-Basin, sample B1775 was attributed to the 'Transitional Formation', a sandstone unit that can be correlated to the sandstone beds that predate deposition of the Chipanga Seam. This sandstone unit is known as the Cambéua Sandstone in the Moatize Coalfield (Real, 1966; Lopes et al., 2021a) and can be correlated with samples SC2X-DH00011/D33 and SC2X-DH00011/A62 of the Moatize Coalfield in this study. Most zircon grains in sample B1775 have U-Pb zircon ages of 1172–1021 Ma, with a peak at 1100 Ma. There are also subpopulations at 1256–1244 Ma and 1544–1474 Ma. The primary zircon population in sample B1775 matches with the equivalent Moatize Formation samples of the N'Condédzi Coalfield, which are also dominated by a unimodal zircon population at 1100–950 Ma, suggesting that the Chicôa-Mecúcoè sub-basin and the N'Condédzi Coalfield had similar sediment source regions during the deposition of the Moatize Formation. However, the absence of zircons with ages ranging from 610 to 490 Ma and 900–780 Ma, which are common in the lower part of the Moatize Formation in the Moatize Coalfield, suggests that the Chicôa-Mecúcoè sub-basin and the Moatize Coalfield did not share the same sediment source regions during deposition of the Moatize Formation.

5.3.2. Alluvial plain depositional phase associated with the first braided channel belt – early Capitanian to late Wuchiapingian (Fig. 9b)

In the Moatize Coalfield, the samples from the sandstone beds of the first braided channel belt (BENG-DH00005/LD20 and SC2X-DH00027/B02) clearly show three detrital zircon populations (1150–950 Ma, 900–780 Ma and 610–490 Ma). This marks the first time source terranes from the Zambezi Belt, Nampula Block, and possibly from the Southern Irumide Belt (Unango and Marrupa complexes) simultaneously contributed sediment to the alluvial systems of the Moatize Coalfield. This highlights the role of tectonism in the reorganisation of the basin by uplifting and exposing these source terrains to erosion. This implies the uplift of the rift shoulders of the Serra Caroeira Fault, exposing the Zambezi and Báruè Complex, and also the uplift of the Nampula Block.

In the N'Condédzi Coalfield, samples A1TM-058/LD58 and A1TM-058/LD2 were collected from sandstone beds tentatively correlated to the first braided channel belt of the Moatize Coalfield. Their zircon populations range between 1100 and 1000 Ma, indicating that the sediment source was the Southern Irumide Belt terranes located to the north (Tete-Chipata and Malawi Complex) and northeast (Unango and Marrupa complexes) (section 5.2.4). The N'Condédzi Coalfield was not likely sourced from the Zambezi Belt or the Nampula Block due to the absence of 610–490 Ma and 900–780 Ma zircon populations, which are always present in the equivalent sandstone units of the Moatize Coalfield. This suggests the presence of a topographic barrier between the two coalfields during the mid-Guadalupian. We suggest that this physical barrier between the two depocenters was an intra-rift horst block (likely Mesoproterozoic Tete Suite rocks) that persisted until the end Permian.

Sample BENG-DH00005/LD21 located stratigraphically above the first braided channel belt, was collected from a sandstone bed whose sedimentary structures indicate a reduction in energy in the alluvial setting and a shift to more mixed load (meandering) river systems (Fernandes et al., 2023) The zircon population in this sample reflects another important change in the sediment source region(s). The absence of the 900–780 Ma population indicates that the Zambezi Belt was no longer a sediment source, as it was the only source area with exclusively that age range. Instead, the bimodal zircon population of 1150–950 Ma and 610–490 Ma implies the upper part of the Moatize Formation was sourced from the Nampula Block with a minor contribution from the Zambezi Belt, located to the east and south of this coalfield, respectively. The available palaeocurrent data from channel-fill sandstones in this part of the Moatize Formation (Bicca et al., 2017; Key et al., 2015; Mugabe, 1999; Pendkar et al., 2014) indicates that the rivers flowed mainly to the west and southwest, which supports the sediment transport directions inferred from the detrital zircon provenance analysis, particularly the uplift of the Nampula Block, which acted as the main sediment source.

5.3.3. Alluvial plain depositional phase associated with the second braided channel belt – early Changhsingian to latest Changhsingian (Fig. 9b)

This depositional phase starts with a thick sandstone interval deposited in a braided channel system related to a renewed phase of tectonism in the basin (Fernandes et al., 2023). This phase coincides typically with the first occurrence of the spore *Osmundacidites senectus* associated with the development of the Grande Falésia coal seam and marks the base of the Matinde Formation (Pereira et al., 2019; Lopes et al., 2020; Fernandes et al., 2023).

In the Moatize Coalfield, samples SC2X-DH00011/D34, SC2X-DH00010/A63, BENG-DH00005/E81, SC2X-DH00027/B03 and S2B-HQ051/C23 were collected from this second braided channel belt. From these samples, only sample BENG-DH00005/E81 has three zircon populations (1150–950 Ma, 900–780 Ma and 610–490 Ma). The other samples show only two zircon populations at 1150–950 Ma and 610–490 Ma. This again suggests that during the tectonic pulses associated with the deposition of the braided channel belts, more areas were exposed as sediment sources, particularly from the Zambezi Belt, implying vertical movements along the Serra Carroeira Fault. However, the exposure of the Zambezi Belt was transient since no 900–780 Ma zircons are found in sandstones above this braided channel belt. Except for sample E81, the detrital zircon data imply that the source area for the Matinde Formation in the Moatize Coalfield was the Nampula Block.

In the N'Condédzi Coalfield, the Matinde Formation is represented by samples A1TM-058/LD22, A1TM-058/LD60, A1TM-058/LD3, and CIMT-014/LD14. Sample A1TM-058/LD22 is tentatively correlated to the second braided channel belt of the Moatize Coalfield at the top of the Grande Falésia Seam. The LD14 sample represents the last sand bed deposited before the Permo-Triassic Boundary in this coalfield (Galasso et al., 2019b). The zircon population of all samples shows a single unimodal peak with an age range of 1100–1000 Ma. Again, the absence of 900–780 Ma and 610–490 Ma zircon populations, which are present in the Moatize Coalfield, indicates that the sediment source for N'Condédzi Coalfield remained in the Southern Irumide Belt terranes and that the two coalfields remained isolated from each other during the deposition of the Matinde Formation.

Bicca et al. (2017) published U-Pb zircon ages obtained from a sandstone bed in the Moatize Coalfield near the Serra Caroeira Fault (see Fig. 3), attributed to the Matinde Formation, but indicating a Lower Triassic age. Thus, the conclusions of Bicca et al. (2017) regarding the sediment provenance of this sample were integrated in Fig. 9c which depicts the likely sediment sources during the Lower Triassic.

According to previous data (Bicca et al., 2017), the primary subpopulation ranges from 700 to 490 Ma with peaks at 619 and 628 Ma (Fig. 8). A subpopulation at 900–700 Ma does not have any significant peaks, while a subpopulation at 1260–900 Ma has a peak at 1053 Ma. Our zircon age spectra from the Matinde Formation in the Moatize Coalfield are partially comparable to those of Bicca et al. (2017). However, the zircon subpopulations of these authors have broad age spectra and slightly older peaks. For example, the youngest zircon subpopulation, ranging from 700 to 490 Ma, has 628 Ma and 619 Ma peaks, whereas our youngest zircon subpopulation ranges between 610 and 490 Ma, with a main peak at ca. 530 Ma. Only one of our samples from the Matinde Formation in the Moatize Coalfield (BENG-DH00005/E81) exhibits three zircon subpopulations, similar to that of Bicca et al. (2017). The source terrain inferences of these previous data align with those of this study, which include the Guro Suite of the Zambezi Belt, the Nampula Block, and the Southern Irumide Belt units of the Unango and Marrupa complexes.

The Matinde Formation in the Chicôa-Mecúcoè Sub-Basin yields a main detrital zircon population at 1259–1022 Ma, with a peak at 1104 Ma, with subpopulations at 996–705 Ma and 607–525 Ma (Whitecross, 2020). The Whitecross (2020) sample (B1766) was taken from the lower part of the Matinde Formation from a horizon that probably represents the braided channel belt. The zircon age spectra show a strong correlation with sample BENG-DH00005/E81 from the Matinde Formation in the Moatize Coalfield but not with the Matinde Formation in the N'Condédzi Coalfield which has a unimodal 1100–950 Ma population. The similar detrital zircon spectra and stratigraphic position of samples B1766 of Whitecross (2020) and BENG-DH00005/E81 from the Moatize Coalfield further supports the influence of tectonic activity during the onset of Matinde Formation deposition in both Karoo depocenters. Whitecross (2020) attributes a likely sediment source region for sample B1766 to the Zambezi Belt to the south and the Southern Irumide Belt to the north and northeast.

5.3.4. Alluvial plain depositional phase associated with the Lower Triassic Cádzi Formation – early Induan to late Olenekian (Fig. 9c)

The Lower Triassic sandstones of the Cádzi Formation were investigated only in the N'Condédzi Coalfield. Six sandstone beds were sampled from borehole CIMT-014 (CIMT-014/LD11, CIMT-014/LD12, CIMT-014/LD15, CIMT-014/LD16, CIMT-014/LD17 and CIMT-014/LD19). No Middle Triassic rocks are recognised in the N'Condédzi Coalfield, and the contact between the Lower and the Upper Triassic sedimentary rocks could correspond to a major hiatus (Galasso et al., 2019b).

All samples except for CIMT-014/LD15 are dominated by a zircon population at 1100–1000 Ma. In sample CIMT-014/LD15, the primary zircon population is 650–490 Ma with a peak at 610 Ma. In all other samples, the 650–490 Ma zircon population is minor and is associated with thick coarse-grained sandstone intervals, which probably correspond to channel-fill deposits of braided rivers (e.g. CIMT-014/LD11, CIMT-014/LD16 and CIMT-014/LD15). The Lower Triassic zircon spectra point to a sediment source in the Southern Irumide Belt located to the north of this coalfield, with 650–490 Ma zircon population linked to Pan-African intrusive rocks in the late Mesoproterozoic mobile belt. However, the link between the 650–490 Ma zircon population and thick and coarse-grained sandstone and conglomerate intervals can be tentatively ascribed to Early Triassic tectonic pulses in the Metangula Graben in Niassa province (Verniers et al., 1989) and in the Karoo basins of Tanzania (Wopfner, 2002). An alternative explanation for the presence of the 490–650 Ma zircon population in the Lower Triassic sandstones is the regional devastation of vegetation due to the catastrophic end-Permian climatic upheaval (Aftabuzzaman et al., 2021; Benton and Newell, 2014; Chen et al., 2022; Retallack, 2021). Vegetation collapse resulted in the development unprotected soils in the catchment areas which were more prone to erosion. This may have caused a denser drainage network that, together with uplift caused by tectonism, triggered the expansion of the catchment areas into the Pan-African granitoid and syenite intrusions present in the Tete-Chipata Terrane (e.g., Macanga Granite at ca. 470 Ma, Sinda Suite at ca. 502 Ma, Ulónguè Suite at ca. 570 Ma).

5.3.5. Alluvial plain depositional phase associated with the Upper Triassic Cádzi Formation – Carnian (Fig. 9d)

The three samples from the Upper Triassic (Carnian) (A1TM-039/LD9, A1TM-039/LD10, CIMT-014/LD13, exhibit a single zircon population at 1100–1000 Ma. This indicates that the sediment source for these samples was from the Southern Irumide Belt (Tete-Chipata Terrane and the Malawi Unango and Marrupa complexes). The Southern Irumide Belt was, therefore, the primary source of sediment from the Upper Permian to the Upper Triassic in the N'Condédzi coalfield.

6. Conclusions

Our detrital zircon U-Pb geochronology study on the Moatize and N'Condédzi coalfields in the ZKBM enables the following conclusions to be drawn regarding its provenance, sediment dispersal pathways and basin evolution:

- The boreholes from the two coalfields reveal a stratigraphy that ranges from the early Roadian (lower Guadalupian) to the Carnian (early Upper Triassic). However, it is only possible to correlate the

Permian strata between the two coalfields, as the boreholes in the Moatize Coalfield did not intersect any Triassic strata.

- The detrital zircon spectra in the Permian samples of the Moatize Coalfield define three subpopulations at 1150–950 Ma, 900–780 Ma and 650–490 Ma; detrital zircons outside these age ranges are rare. In contrast, the detrital zircon spectra in the N'Condédzi Coalfield define a unimodal population at 1150–950 Ma. This indicates that the sediment source regions were proximal and located in the Pan-African and Mesoproterozoic mobile belts adjacent to the coalfields, namely the Zambezi Belt (Guro Suite, Báruè Complex), the Southern Irumide Belt (Tete-Chipata Terrane, Malawi, Unango and Marrupa Complexes), and the Nampula Block.
- The detrital zircon age spectra of the Moatize and N'Condédzi coalfields indicate provenance regions in the adjacent Precambrian to early Cambrian terranes. This agrees with the general tectonic style described for intracontinental rift basins, which are characterised by proximal sediment source regions and small catchment areas.
- During the Permian, the source region for the N'Condédzi Coalfields was the Tete-Chipata Terrane and Malawi Complex (1150–950 Ma) to the north-northeast of the coalfield and remained the same, despite changes in depositional settings and pulses of enhanced tectonic activity. The successive movements along the Mwanza Fault were the main structural element that controlled the sediment sources of this coalfield. The Moatize Coalfield recorded more variability in the location of the source regions in the Permian. During the initial lake delta depositional setting related to the deglacial phase, the detrital zircon population indicated main provenance in the Zambezi Belt (900–780 Ma) to the south and minor sourcing from the Nampula Block (1150–950 Ma and 650–490 Ma) to the east. This indicates that there was uplift of the Zambezi Belt at the rift shoulders of the Serra Caroeira Fault, thus creating positive relief that acted as the main sediment source area. The change from lake delta to alluvial deposition is attributed to a major tectonic phase in the basin that lead to the reorganisation of the source areas (Fernandes et al., 2023). It is marked by a thick early Capitanian sandstone interval above the Chipanga Seam that is interpreted as a braided channel. There is an accompanying change in detrital zircon provenance within the first braided channel belt, with an equal provenance contribution from the Zambezi Belt and the Nampula Block (populations at 1150–950 Ma, 900–780 Ma and 650–490 Ma). This the uplifting Nampula Block started to act as an important sediment source area.
- The sandstone samples above the first braided channel belt are dominated by two detrital populations (1150–950 Ma and 650–490 Ma) that can be attributed to the Nampula Block. The near absence of the Zambezi Belt detrital zircon population (900–780 Ma) in the sandstones indicates a significant change in the main source areas, with tectonic uplift of the Nampula Block east of the Moatize Coalfield the likely cause. These results agree with previous paleocurrent studies from channel-bar sandstones in the Moatize region, which indicate main paleoflows to the west (Mugabe, 1999; Bicca et al., 2017).
- The absence of 900–780 Ma and 650–490 Ma detrital zircon populations in the N'Condédzi Coalfield suggests that these two Karoo sub-basins were not interconnected during the mid-to late Permian. This implies that these basins functioned as separate depocenters separated by a physical barrier, likely an intra-rift horst of the Mesoproterozoic Gabbro – Anorthosite Tete Suite. This barrier may have been significant, extending eastwards into the Lúrio Belt. To the south of the Lúrio Belt, the primary drainage flow would have been towards the west, while to the north of the Lúrio Belt, the drainage flow would have predominantly towards the south-southwest.
- The Lower Triassic sample from the Moatize Coalfield of Bicca et al. (2017), indicates sediment source from the Guro Suite of the Zambezi Belt, the Nampula Block, and the Southern Irumide Belt units of the Unango and Marrupa complexes
- In the Lower Triassic sandstones of the N'Condédzi Coalfield, the prominent detrital zircon population is 1150–950 Ma, indicating sourcing from the Tete-Chipata Terrane and Malawi Complex. A minor 650–490 Ma population can be explained by tectonic pulses along the Mwanza Fault, resulting in braided channel deposition of thick units of coarse-grained sandstones deposited in braided channel belts, and the end-Permian environmental and climatic disturbances. The latter resulted in the sudden loss of vegetation making the soils in the sediment source areas more exposed and prone to erosional processes. This, in turn, led to a denser fluvial network and an increase in the extension of the drainage basins located on the rift shoulders of the Mwanza Fault. The expansion of the drainage basin areas, both upstream and laterally, may have intersected exposures of Pan-African intrusive in the Tete-Chipata Terrane and the Malawi and Unango complexes, which were the source terranes of the 650–490 Ma detrital zircon population.
- The Upper Triassic sandstones yield a unimodal 1150–950 Ma detrital zircon population, implying a return to the sediment routing system that characterised the basin during the mid to late Permian, with sourcing from the Tete-Chipata Terrane and Malawi Complex and controlled by the successive movements of the Mwanza Fault. Further insights into the Triassic compartmentation or interconnection of different depocenters can be obtained from future detrital zircon studies on other Karoo depocenters of the ZKBM.

CRediT authorship contribution statement

Paulo Fernandes: Writing – review & editing, Writing – original draft, Visualization, Validation, Supervision, Project administration, Methodology, Investigation, Funding acquisition, Formal analysis, Conceptualization. **Raul C.G.S. Jorge:** Writing – review & editing, Validation, Investigation, Formal analysis. **Luís Albardeiro:** Writing – review & editing, Validation, Resources, Methodology, Investigation, Formal analysis, Data curation. **David Chew:** Writing – review & editing, Validation, Resources, Methodology, Investigation, Formal analysis. **Foteini Drakou:** Writing – review & editing, Validation, Methodology, Investigation, Formal analysis. **Zélia Pereira:** Writing – review & editing, Validation, Investigation, Formal analysis, Data curation. **João Marques:** Writing – review & editing, Writing – original draft, Validation, Methodology, Investigation, Formal analysis, Conceptualization.

Declaration of Competing Interest

The authors declare the following financial interests/personal relationships which may be considered as potential competing interests: Paulo Fernandes reports financial support was provided by Foundation for Science and Technology (Portugal). If there are other authors, they declare that they have no known competing financial interests or personal relationships that could have appeared to influence the work reported in this paper.

Acknowledgements

This work was supported by the project PALEOCLIMOZ (PTDC/CTA-GEO/30082/2017), Fundação para a Ciência e Tecnologia (FCT), Portugal, and by FCT projects LA/P/0069/2020, awarded to the Associate Laboratory ARNET, UIDP/00350/2020, awarded to CIMA of the University of the Algarve (https://doi.org/10.54499/UIDP/00350/2020), and UIDB/50019/2020-IDL of the Portuguese national funds (PIDDAC). D. Chew acknowledges support from Science Foundation Ireland through research grants 13/RC/2092_P2 (iCRAG Research Centre). The manuscript has been greatly improved by the contributions of two anonymous reviewers. P. Fernandes wishes to thank Vulcan Moatize Mine Moçambique and Coal India for access to the core and data

for the boreholes and for permission to publish this work, and all the Gondwana staff from the Tete office, namely Alfredo Tembo, Tomé Eneia, Jorge Bettencourt and Humberto Lobo, for their help over the last few years.

Appendix A. Supplementary data

Supplementary data to this article can be found online at https://doi.org/10.1016/j.jafrearsci.2024.105458.

Data availability

Data will be made available on request.

References

Achimo, M., Vasconcelos, L., Marques, J., Ferrara, M., 2014. Sedimentologia dos depósitos tilíticos do vale do Rio Murrongódzi, Bacia Carbonífera de Moatize – Minjova, Tete, Moçambique, 2° Congresso Nacional de Geologia e 12° Congresso de Geoquímica dos Países de Língua Portuguesa. Maputo, Moçambique 57–61.

Afonso, R.S., 1984. Ambiente geológico dos carvões gonduânicos de Moçambique - uma síntese. In: Lemos de Sousa, M.J. (Ed.), Symposium on Gondwana Coals, Lisbon, 1983. Proceedings and Papers, vol. 70. Comum. Serv. Geol. Portugal, pp. 205–214.

Afonso, R.S., Marques, J.M., Ferrara, M., 1998. Evolução Geológica de Moçambique. Instituto de Investigação Científica Tropical de Portugal and Direcção Nacional de Geologia de Moçambique. Lisboa, Portugal.

Aftabuzzaman, M., Kaiho, K., Biswas, R.K., Liu, Y., Saito, R., Tian, L., Bhat, G.M., Chen, Z.-Q., 2021. End-Permian terrestrial disturbance followed by the complete plant devastation, and the vegetation proto-recovery in the earliest-Triassic recorded in coastal sea sediments. Global Planet. Change 205, 103621.

Ashwal, L.D., Armstrong, R.A., Roberts, R.J., Schmitz, M.D., Corfu, F., Hetherington, C.J., Burke, K., Gerber, M., 2007. Geochronology of zircon megacrysts from nepheline-bearing gneisses as constraints on tectonic setting: implications for resetting of the U-Pb and Lu-Hf isotopic systems. Contrib. Mineral. Petrol. 153, 389–403.

Barham, M., Kirkland, C.L., Handoko, A.D., 2022. Understanding ancient tectonic settings through detrital zircon analysis. Earth Planet Sci. Lett. 583, 117425.

Benton, M.J., Newell, A.J., 2014. Impacts of global warming on Permo-Triassic terrestrial ecosystems. Gondwana Res. 25, 1308–1337.

Bicca, M.M., Philipp, R.P., Jelinek, A.R., Ketzer, J.M.M., Scherer, C.M.D., Jamal, D.L., dos Reis, A.D., 2017. Permian-early triassic tectonics and stratigraphy of the Karoo Supergroup in northwestern Mozambique. J. Afr. Earth Sci. 130, 8–27.

Bingen, B., Jacobs, J., Viola, G., Henderson, I.H.C., Skår, Ø., Boyd, R., Thomas, R.J., Solli, A., Key, R.M., Daudi, E.X.F., 2009. Geochronology of the Precambrian crust in the Mozambique belt in NE Mozambique, and implications for Gondwana assembly. Precambrian Res. 170, 231–255.

Catuneanu, O., Wopfner, H., Eriksson, P.G., Cairncross, B., Rubidge, B.S., Smith, R. M.H., Hancox, P.J., 2005. The Karoo basins of south-central Africa. J. Afr. Earth Sci. 43, 211–253.

Cawood, P.A., Hawkesworth, C.J., Dhuime, B., 2012. Detrital zircon record and tectonic setting. Geology 40, 875–878.

Chaúque, F.R., 2012. Contribuição para o conhecimento da evolução tectônica do Cinturão de Moçambique, em Moçambique. Universidade de São Paulo, São Paulo. https://doi.org/10.11606/T.44.2012.tde-02062015-152355. PhD Thesis, Instituto de Geociências.

Chaúque, F.R., Cordani, U.G., Jamal, D.L., 2019. Geochronological systematics for the Chimoio-Macossa frontal nappe in central Mozambique: implications for the tectonic evolution of the southern part of the Mozambique belt. J. Afr. Earth Sci. 150, 47–67.

Chen, Z.-Q., Harper, D.A.T., Grasby, S., Zhang, L., 2022. Catastrophic event sequences across the Permian-Triassic boundary in the ocean and on land. Global Planet. Change 215, 103890.

Council for Geoscience, 2007. Map Explanation: Sheets 1537 Alto Molócuè, 1538 Murrupula, 1539 Nampula, 1540 Mogincual, 1637 Errego, 1638 Gilé and 1639–40 Angoche, Ministério dos Recursos Minerais e Energia, Direcção Nacional de Geologia. Maputo, Mozambique and Council for Geoscience, Pretoria, South Africa, pp. 1–392.

Dickinson, W., 2008. Impact of differential zircon fertility of granitoid basement rocks in North America on age populations of detrital zircons and implications for granite petrogenesis. Earth Planet Sci. Lett. 275, 80–92. https://doi.org/10.1016/j.epsl.2008.08.003.

Evans, R.J., Ashwal, L.D., Hamilton, M.A., 1999. Mafic, ultramafic and anorthositic rocks of the Tete Complex, Mozambique: petrology, age and significance. S. Afr. J. Geol. 102, 153–166.

Fernandes, P., Hancox, P.J., Mendes, M., Pereira, Z., Lopes, G., Marques, J., Jorge, R.C.G.S., Albardeiro, L., 2023. The age and depositional environments of the lower Karoo Moatize Coalfield of Mozambique: insights into the postglacial history of central Gondwana. Palaeoworld. https://doi.org/10.1016/j.palwor.2023.07.001.

Galasso, F., Fernandes, P., Montesi, G., Marques, J., Spina, A., Pereira, Z., 2019a. Thermal history and basin evolution of the Moatize - minjova Coal Basin (N'Condédzi sub-basin, Mozambique) constrained by organic maturation levels. J. Afr. Earth Sci. 153, 219–238.

Galasso, F., Pereira, Z., Fernandes, P., Spina, A., Marques, J., 2019b. First record of permo-triassic palynomorphs of the N'condédzi sub-basin, Moatize-Minjova coal basin, Karoo Supergroup, Mozambique. Rev. Micropaleontol. 64, 100357.

Goscombe, B., Foster, D.A., Gray, D., Wade, B., 2020. Assembly of central Gondwana along the Zambezi belt: metamorphic response and basement reactivation during the Kuunga Orogeny. Gondwana Res. 80, 410–465.

Grantham, G., Macey, P., Ingram, B., Roberts, M., Rohwer, M., Opperman, R., Manhica, V., Alvares, S., Bacalhau, C., Du Toit, M., 2007. Map Explanation of Sheets Meconta (1439) and Nacala (1440). National Directorate of Geology, Republic of Mozambique, p. 240.

Grantham, G., Marques, J., Wilson, M., Manhiça, V., Hartzer, F., 2011. Explanation of the Geological Map of Mozambique, Scale 1: 1 000 000. Ministério Dos Recursos Minerais. Direcção Nacional de Geologia, p. 383.

Grantham, G.H., Macey, P., Ingram, B., Roberts, M., Armstrong, R., Hokada, T., Shiraishi, K., Jackson, C., Bisnath, A., Manhiça, V., 2008. Terrane correlation between Antarctica, Mozambique and Sri Lanka; comparisons of geochronology, lithology, structure and metamorphism and possible implications for the geology of southern Africa and Antarctica. Geol. Soc. Spec. Publ. 308, 91–119.

GTK Consortium, 2006. Map Explanation; Volume 2: Sheets 1630 – 1934. Geology of Degree Sheets Mecumbura, Chioco, Tete, Tambara, Guro, Chemba, Manica, Catandica, Gorongosa, Rotanda, Chimoio and Beira, Mozambique. Ministério Dos Recursos Minerais. Direção Nacional de Geologia, Maputo, pp. 1–411, 4 apêndices.

Hanson, R.E., 2003. Proterozoic geochronology and tectonic evolution of southern Africa. Geol. Soc. Spec. Publ. 206, 427–463.

Hanson, R.E., Wilson, T.J., Wardlaw, M.S., 1988. Deformed batholiths in the Pan-African Zambezi belt, Zambia: age and implications for regional Proterozoic tectonics. Geology 16, 1134–1137.

Hargrove, U.S., Hanson, R.E., Martin, M.W., Blenkinsop, T.G., Bowring, S.A., Walker, N., Munyanyiwa, H., 2003. Tectonic evolution of the Zambezi orogenic belt: geochronological, structural, and petrological constraints from northern Zimbabwe. Precambrian Res. 123, 159–186.

Hartzer, F.J., Manhiça, V.J., Marques, J.M., Grantham, G., Cune, G.R., Feitio, P., Daudi, E.X.F., 2008. Carta Geológica de Moçambique na escala 1:1000000. Direcção Nacional de Geologia, Ministério dos Recursos Minerais, Maputo, Moçambique.

Jacobs, J., Bingen, B., Thomas, R.J., Bauer, W., Wingate, M.T., Feitio, P., 2008. Early Palaeozoic orogenic collapse and voluminous late-tectonic magmatism in Dronning Maud Land and Mozambique: insights into the partially delaminated orogenic root of the East African–Antarctic Orogen? Geol. Soc. Spec. Publ. 308, 69–90.

Jamal, D.L., 2005. Crustal Studies across Selected Geotransects in NE Mozambique: Differentiating between Mozambican (~ Kibaran) and Pan-African Events, with Implications for Gondwana Studies. University of Cape, Town, pp. 1–730.

Johnson, S.P., De Waele, B., Liyungu, K.A., 2006. U-Pb sensitive high-resolution ion microprobe (SHRIMP) zircon geochronology of granitoid rocks in eastern Zambia: terrane subdivision of the Mesoproterozoic Southern Irumide Belt. Tectonics 25, 1–29.

Johnson, S.P., Rivers, T., Waele, B.D., 2005. A review of the Mesoproterozoic to early Palaeozoic magmatic and tectonothermal history of south–central Africa: implications for Rodinia and Gondwana. J. Geol. Soc. 162, 433–450.

Johnson, S.P., Waele, B.D., Evans, D., Banda, W., Tembo, F., Milton, J.A., Tani, K., 2007. Geochronology of the Zambezi supracrustal sequence, southern Zambia: a record of neoproterozoic divergent processes along the southern margin of the Congo craton. J. Geol. 115, 355–374.

Katongo, C., Koller, F., Kloetzli, U., Koeberl, C., Tembo, F., Waele, B.D., 2004. Petrography, geochemistry, and geochronology of granitoid rocks in the Neoproterozoic-Paleozoic Lufilian–Zambezi belt, Zambia: implications for tectonic setting and regional correlation. J. Afr. Earth Sci. 40, 219–244.

Key, R.M., Cotterill, F.P.D., Moore, A.E., 2015. The Zambezi River: an archive of tectonic events linked to the amalgamation and disruption of Gondwana and subsequent evolution of the African plate. S. Afr. J. Geol. 118, 425–438.

Kröner, A., Sacchi, R., Jaeckel, P.T., Costa, M., 1997. Kibaran magmatism and Pan-African granulite metamorphism in northern Mozambique: single zircon ages and regional implications. J. Afr. Earth Sci. 25, 467–484.

Kröner, A., Willner, A.P., Hegner, E., Jaeckel, P., Nemchin, A., 2001. Single zircon ages, PT evolution and Nd isotopic systematics of high-grade gneisses in southern Malawi and their bearing on the evolution of the Mozambique belt in southeastern Africa. Precambrian Res. 109, 257–291.

Lopes, G., Pereira, Z., Fernandes, P., Marques, J., Mendes, M., Gotz, A.E., 2021a. Permian stratigraphy and palynology of the lower Karoo group in Mozambique - a 2020 perspective. Newsl. Stratigr. 54, 335–362.

Lopes, G., Pereira, Z., Fernandes, P., Mendes, M., Marques, J., Jorge, R.C.G.S., 2021b. Late permian palaeoenvironmental evolution of the Matinde Formation in the Muarádzi Sub-basin, Moatize-Minjova basin, Mozambique. J. Afr. Earth Sci. 176, 104138.

Ludwig, K.R., 2003. User's Manual for Isoplot 3.00: a Geochronological Toolkit for Microsoft Excel, vol. 4. Berkeley Geochronology Center Special Publication, p. 4.

Macey, P.H., Ingram, B.A., Cronwright, M.S., Botha, G.A., Roberts, M.R., Grantham, G. H., Maree, L.P., Botha, P.M.W., Kota, M., Opperman, R., Haddon, I.G., Nolte, J.C., Rower, M., 2007. Map explanation of sheets Alto Molócuè (1537). Murrupula (1538), Nampula (1539), Mogincual (1540), Errego (1637), Gilé (1638) and Angoche (1639-40) National Directorate of Geology, Republic of Mozambique.

Macey, P.H., Thomas, R.J., Grantham, G.H., Ingram, B.A., Jacobs, J., Armstrong, R.A., Roberts, M.P., Bingen, B., Hollick, L., de Kock, G.S., Viola, G., Bauer, W., Gonzales, E., Bjerkgård, T., Henderson, I.H.C., Sandstad, J.S., Cronwright, M.S., Harley, S., Solli, A., Nordgulen, Ø., Motuza, G., Daudi, E., Manhiça, V., 2010. Mesoproterozoic geology of the Nampula block, northern Mozambique: tracing

fragments of Mesoproterozoic crust in the heart of Gondwana. Precambrian Res. 182, 124–148.
Macey, P.H., Miller, J.A., Rowe, C.D., Grantham, G.H., Siegfried, P., Armstrong, R.A., Kemp, J., Bacalau, J., 2013. Geology of the Monapo klippe, NE Mozambique and its significance for assembly of central Gondwana. Precambrian Res. 233, 259–281.
Manda, B.W.C., Cawood, P.A., Spencer, C.J., Prave, T., Robinson, R., Roberts, N.M.W., 2019. Evolution of the Mozambique Belt in Malawi constrained by granitoid U-Pb, Sm-Nd and Lu-Hf isotopic data. Gondwana Res. 68, 93–107.
Mange, M.A., Maurer, H.F.W., 1992. Heavy Minerals in Colour. Chapman & Hall, London, p. 147. https://doi.org/10.1007/978-94-011-2308-2.
Manhiça, A., Grantham, G.H., Armstrong, R., Guise, P., Kruger, F., 2001. Polyphase deformation and metamorphism at the Kalahari craton—Mozambique belt boundary. Geol. Soc. Spec. Publ. 184, 303–322.
Manjate, V.A., 2012. Geocronologia da região de Gondola-Nhamatanda (Centro de Moçambique). Instituto de Geociências, Universidade de São Paulo. https://doi.org/10.11606/D.44.2012.tde-21122012-085416. MsC Thesis.
Manjate, V.A., 2015. Caracterização geocronologica dos granitoides do Complexo de Barue e da Suite de Guro, centro-oeste de Moçambique: implicações tectonicas e metalogenéticas. IGc/USP, São Paulo, p. 142. PhD Thesis.
Manjate, V.A., Tassinari, C.C.G., 2018. Zircon U–Pb geochronology and Nd isotope systematics of the Guro Suite granitoids, Mozambique: Implications for Neoproterozoic crust reworking events. J. Afr. Earth Sci. 148, 69–79.
Mäntäri, I., 2008. Mesoarchaean to Lower Jurassic U-Pb and Sm-Nd Ages from NW Mozambique. Special Paper, vol. 48. Geological Survey of Finland, pp. 81–119.
Mariga, A.J., Hanson, R.E., Martin, M.W., Singletary, S.J., Owring, S.A., 1998. Timing of polyphase ductile deformation at deep to mid-crustal levels in the Neoproterozoic Zambezi belt, NE Zimbabwe. Geol Soc Am. Abstracts with Programs 30, A292.
Midwinter, D., Hadlari, T., Dewing, K., Matthews, W.A., 2024. Disruption and localization of sediment pathways by continental extension: detrital-zircon provenance change from upper Triassic to lower Jurassic in the northern Sverdrup Basin, Nunavut. Geol. Mag. 1–10.
Mugabe, J.A., 1999. Karoo Deposits of Zambezi Graben - Moatize and Tete City Mozambique; Sedimentary Facies Distribution and Palynological Approach. University of Utrecht, Netherlands, p. 297.
Nasdala, L., Corfu, F., Schoene, B., Tapster, S.R., Wall, C.J., Schmitz, M.D., Ovtcharova, M., Schaltegger, U., Kennedy, A.K., Kronz, A., Reiners, P.W., Yang, Y.-H., Wu, F.-Y., Gain, S.E.M., Griffin, W.L., Szymanowski, D., Chanmuang, N.C., Ende, M., Valley, J.W., Spicuzza, M.J., Wanthanachaisaeng, B., Giester, G., 2018. GZ7 and GZ8 – two zircon reference materials for SIMS U-Pb geochronology. Geostand. Geoanal. Res. 42, 431–457.
Norconsult Consortium, 2007. Sheet Explanation, Report No. B6.f: Sheets 1039 Muidine, 1040 Palma, 1134 Ponta Messuli, 1135 Lupilichi, 1136 Milepa, 1137 Macalange, 1138 Negomano, 1139 Mueda, 1140 Mocímboa da Praia, 1234 Metangula, 1235 Macaloge-Chiconono, 1236 Mavago, 1237 Mecula, 1238 Xixano, 1239 Meluco, 1240 Quissanga-Pemba, 1334 Meponda, 1335 Lichinga, 1336 Majune, 1337 Marrupa, 1338 Namuno, 1339 Montepuez, 1340 Mecúfi, 1435 Mandimba, 1436 Cuamba, 1437 Malema, 1438 Ribáuè-Mecubúri, 1535 Insaca, 1536 Gurúè, 1635 Milange, 1636 Lugela-Mocuba, Geological Mapping – Lot 1. National Directorate of Geology, Ministry of Mineral Resources and Energy, Maputo, Mozambique pp, p. 778.
Orpen, J.L., Swain, C.J., Nugent, C., Zhou, P.P., 1989. Wrench-fault and half-graben tectonics in the development of the Palaeozoic Zambezi Karoo basins in Zimbabwe - the "lower Zambezi" and "Mid-Zambezi" basins respectively - and regional implications. J. Afr. Earth Sci. 8, 215–229.
Paton, C., Hellstrom, J., Bence, P., Woodhead, J., Hergt, J., 2011. Iolite: freeware for the visualisation and processing of mass spectrometric data. J. Anal. At. Spectrom. VL - IS -. online. https://doi.org/10.1039/C1JA10172B.
Pendkar, N., Rubino, J.-L., Jean-Baptiste Baby, G., Sia, S.S.L., Prasetyotomo, W.S., 2014. Lower Karoo sedimentation in Moatize basin, Mozambique: analogue for understanding the deep rift sequence in offshore rovuma basin. International Petroleum Technology Conference, Kuala Lumpur, Malaysia, pp. 1–11.
Pereira, Z., Fernandes, P., Lopes, G., Marques, J., Vasconcelos, L., 2016. The permian-triassic transition in the Moatize-Minjova basin, Karoo Supergroup, Mozambique: a palynological perspective. Rev. Palaeobot. Palynol. 226, 1–19.
Pereira, Z., Fernandes, P., Lopes, G., Marques, J., Vaz, M., Costa, M., Correia, J., Castro, L., Galasso, F., 2019. Palynology of the Muarádzi sub-basin, Moatize-Minjova coal basin, Karoo Supergroup, Mozambique. Rev. Palaeobot. Palynol. 269, 78–93.
Petrus, J.A., Kamber, B.S., 2012. VizualAge: a novel approach to laser ablation ICP-MS U-Pb geochronology data reduction. Geostand. Geoanal. Res. 36, 247–270.
Petry, T.S., Philipp, R.P., Jamal, D.L., Lana, C., Alkmim, A.R., 2022. U-Pb and Lu-Hf zircon data of the grenvilian arc-related Zâmbuè, Fíngoè and Cazula supracrustal complexes, Southern Irumide Belt, NW Mozambique. Precambrian Res. 381, 106860.
Pointon, M.A., Chew, D.M., Ovtcharova, M., Sevastopulo, G.D., Crowley, Q.G., 2012. New high-precision U–Pb dates from western European Carboniferous tuffs; implications for time scale calibration, the periodicity of late Carboniferous cycles and stratigraphical correlation. J. Geol. Soc. 169, 713–721.
Real, F., 1966. Geologia da Bacia do Rio Zambeze (Mocambique). Características geológico-mineiras da Bacia do rio Zambeze em território mocambicano. Junta de Investigacões do Ultramar, Lisboa, Portugal, p. 183.
Retallack, G.J., 2021. Multiple Permian-Triassic life crises on land and at sea. Global Planet. Change 198, 103415.
Sakuwaha, K.u.G., Tsunogae, T., Banda, P., Changasha, C., Sikazwe, O.N., Tsutsumi, Y., 2022. Neoproterozoic thermal events and crustal growth in the Zambezi Belt, Zambia: new insights from geothermobarometry, monazite dating, and detrital zircon geochronology of metapelites. Lithos, 106762.
Sláma, J., Košler, J., Condon, D.J., Crowley, J.L., Gerdes, A., Hanchar, J.M., Horstwood, M.S.A., Morris, G.A., Nasdala, L., Norberg, N., Schaltegger, U., Schoene, B., Tubrett, M.N., Whitehouse, M.J., 2008. Plešovice zircon — a new natural reference material for U–Pb and Hf isotopic microanalysis. Chem. Geol. 249, 1–35.
Song, Y., Ren, J., Liu, K., Lyu, D., Feng, X., Liu, Y., Stepashko, A., 2022. Syn-rift to post-rift tectonic transition and drainage reorganization in continental rifting basins: detrital zircon analysis from the Songliao Basin, NE China. Geosci. Front. 13, 101377.
Thomas, R., Jacobs, J., Horstwood, M., Ueda, K., Bingen, B., Matola, R., 2010. The Mecubúri and Alto Benfica groups, NE Mozambique: aids to unravelling ca. 1 and 0.5 Ga events in the east African orogen. Precambrian Res. 178, 72–90.
Thomas, R.J., Fullgraf, T., Macey, P.H., Boger, S.D., Hölttä, P., Lach, P., Le Roux, P., Dombola, K., Zammit, C., 2022. The mesoproterozoic Nampula subdomain in southern Malawi: completing the story from Mozambique. J. Afr. Earth Sci. 196, 104667.
Tsunogae, T., Uthup, S., Nyirongo, M.W., Takahashi, K., Rahman, M.S., Liu, Q., Takamura, Y., Tsutsumi, Y., 2021. Neoproterozoic crustal growth in southern Malawi: new insights from petrology, geochemistry, and U–Pb zircon geochronology, and implications for the Kalahari Craton–Congo Craton amalgamation. Precambrian Res. 352, 106007.
Vasconcelos, L., Achimo, M., 2010. O carvão em Moçambique. In: Cotelo Neiva, J.M., Ribeiro, A., Mendes Victor, L., Noronha, F., Ramalho, M.M. (Eds.), Ciências Geológicas – Ensino e Investigação da sua História. Geologia das Ex-Colónias de África, pp. 191–206. Lisboa.
Vermeesch, P., 2012. On the visualisation of detrital age distributions. Chem. Geol. 312–313, 190–194.
Verniers, J., Jourdan, P.P., Paulis, R.V., Frasca-Spada, L., De Bock, F.R., 1989. The Karroo graben of Metangula northern Mozambique. J. Afr. Earth Sci. 9, 137–158.
Vinyu, M.L., Hanson, R.E., Martin, M.W., Bowring, S.A., Jelsma, H.A., Krol, M.A., Dirks, P.H.G.M., 1999. U–Pb and 40Ar/39Ar geochronological constraints on the tectonic evolution of the easternmost part of the Zambezi orogenic belt, northeast Zimbabwe. Precambrian Res. 98, 67–82.
Viola, G., Henderson, I.H.C., Bingen, B., Thomas, R.J., Smethurst, M.A., de Azevedo, S., 2008. Growth and collapse of a deeply eroded orogen: insights from structural, geophysical, and geochronological constraints on the Pan-African evolution of NE Mozambique. Tectonics 27, TC5009. https://doi.org/10.1029/2008TC002284.
Westerhof, A.B.P., Lehtonen, M.I., Mäkitie, H., Manninen, T., Pekkala, Y., Gustafsson, B., Tahon, A., 2008. The Tete-Chipata Belt: a new multiple terrane element from Western Mozambique and Southern Zambia. Spec. Pap. Geol. Surv. Finland 2008 (48), 145–166.
Wiecenbeck, M., Allé, P., Corfu, F., Griffin, W.L., Meier, M., Oberli, F., Quadt, A.V., Roddick, J.C., Spiegel, W., 1995. Three natural zircon standards for U-Th-Pb, Lu-Hf, trace element and REE analysis. Geostand. Newsl. 19, 1–23.
Wiedenbeck, M., Hanchar, J.M., Peck, W.H., Sylvester, P., Valley, J., Whitehouse, M., Kronz, A., Morishita, Y., Nasdala, L., Fiebig, J., Franchi, I., Girard, J.-P., Greenwood, R.C., Hinton, R., Kita, N., Mason, P.R.D., Norman, M., Ogasawara, M., Piccoli, P.M., Rhede, D., Satoh, H., Schulz-Dobrick, B., Skår, O., Spicuzza, M., Terada, K., Tindle, A., Togashi, S., Vennemann, T., Xie, Q., Zheng, Y.-F., 2004. Further characterisation of the 91500 zircon crystal. Geostand. Geoanal. Res. 28, 9–39.
Whitecross, L., 2020. Provenance Study on the Karoo Sedimentary Rocks of the Chicôa-Mecúcoè Sub-basin of the Zambezi Basin, Tete Provence, Mozambique: Implications for Basin Development, Sedimentary Processes and Tectonic Controls. MSc Thesis, University of the Witwatersrand, p. 158 (unpubl.).
Wopfner, H., 2002. Tectonic and climatic events controlling deposition in Tanzanian Karoo basins. J. Afr. Earth Sci. 34, 167–177.